Study on the Functions of Protein Phosphatase PPM1D in Myeloid Innate Immunity

骨髄系細胞による自然免疫における

プロテインホスファターゼ PPM1D の機能に関する研究

Laboratory of Biological Chemistry,
Graduate School of Chemical Sciences and Engineering,
Hokkaido University

Fuki Kudoh

2020

abbreviations

AML	acute myeloid leukamia
APC	antigen presenting cell
ATRA	all-*trans* retinoic acid
CD	cluster of differentiation
CEBPE	CCAAT/enhancer binding protein epsilon
CFSE	5-(and-6)-Carboxyfluorescein diacetate succinimidyl ester
COX-1/2	cyclooxygenase-1/2
DAG	diacylglycerol
DEFA	Alpha defensin
DEG	Differential Expression Gene
ERK	Extracellular Signal-regulated Kinase
FATP2	Fatty Acid Transport Protein 2
FBS	Fetal Bovine Serum
FCΓR	Fc region of immunoglobulins gamma
FDR	False Discovery Rate
FITC	Fluorescein isothiocyanate
HPRT	Hypoxanthine phosphoribosyltransferase
HSC	Hematopoietic stem cell
IFNγ	Interferon gamma
IL	Interleukin
LPS	Lipopolysaccharide
MAPK	Mitogen-activated Protein Kinase
MDS	Myelodysplastic syndromes
mPGES-1/2	Microsomal prostaglandin E synthase-1/2
RNA	ribonucleic acid
NBT	Nitroblue tetrazolium
NLS	Nuclear localization signal
PCR	polymerase chain reaction
PGE_2	prostaglandin E2
PMN	polymorphonuclear neutrophils

PMN-MDSC	PMN-Myeloid-derived suppressor cell
PPARG	Peroxisome proliferator-activated receptor gamma
PPM1D	Mg2+- or Mg2+-dependent protein phosphatase 1, delta
PRR	pattern recognition receptor
ROS	reactive oxygen species
RPMI	Roswell Park Memorial Institute medium
SD	standard deviation
SLE	systemi lupus erythematosus
TAP	1, 3a, 6a-triazapentalene
TNFα	Tumor necrosis factor
TP53	cellular tumor antigen p53

1. General Introduction

1.1. Immunity

1.1.1. Innate immunity

Humans are always at a risk of infection. Thus, immune responses, whereby the immune system defends individuals from harmful pathogens, are a critical process that protects live. The vertebrates' immune system can be divided into two groups: innate immunity and adaptive immunity. Both recognize non-self and remove non-self only. The innate immune response is an immediate and broad-specific response against genetically conserved pathogens. Innate immunity is mediated by somatic cells and myeloid cells (**Figure 1-1**)[1]. Somatic cells express pattern recognition receptors (PRRs) that activate immune cells by paracrine. For example, Lipopolysaccharide (LPS), containing a Gram-negative bacterial cell wall is recognized by Toll-like receptor 4 (TLR4), a PRR, which upon activation propagates intracellular signals via the PI3K, MAPK, and IKKs pathways. These pathways promote gene transcription by NF-κB, AP-1 and IRF3, which trigger the secretion of inflammatory cytokines such as IL-1β and IFN-γ [2−4].

Of note, innate myeloid cells are activated directly by cytokines or by pathogen-associated molecular patterns such as LPS[5]. The first line of host defense is neutrophils, the most abundant myeloid cell in the peripheral blood. Activated neutrophils migrate into sites of infection or damaged tissues and directly remove pathogens by phagocytosis or the secretion of enzymes. Chronic inflammation induces anti-inflammatory compounds to limit pain and damage to the host[6]. Prostaglandin E_2 (PGE_2) is an eicosanoids and is essential for the resolution of neutrophil-induced inflammation [7].

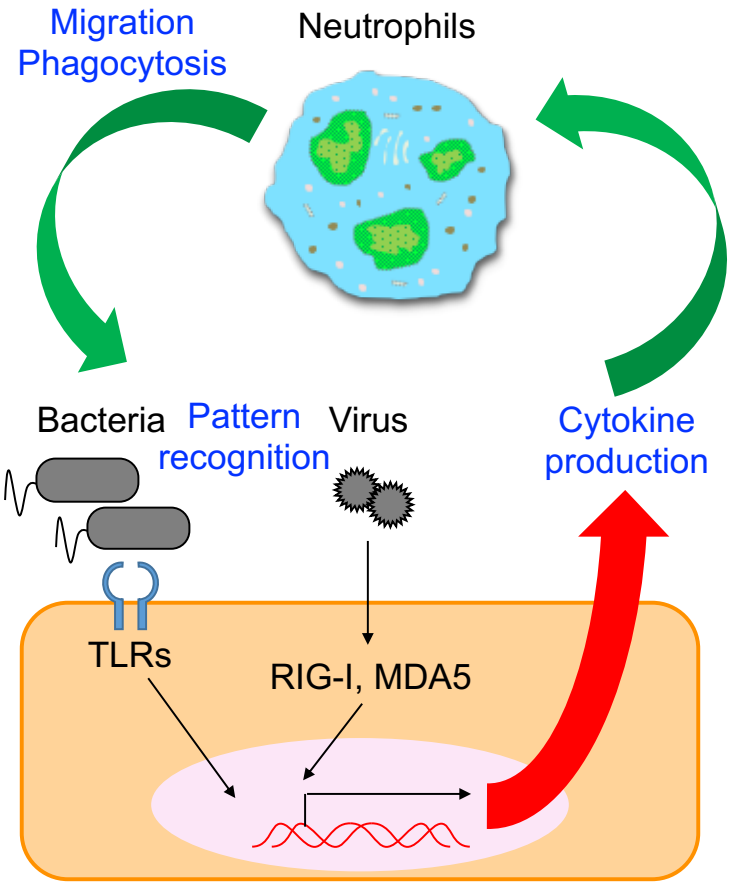

Figure 1-1 Somatic cells and leukocyte interaction in innate immunity

Somatic cells recognize the pathogens by pattern recognition. PRRs propagate signals and produce cytokines or other mediators. Innate myeloid cells are activated by cytokines from somatic cells and other immune cells.

1.1.2. Myeloid differentiation and acute myelocytic leukemia

Myeloid differentiation is tightly regulated. Neutrophils are differentiated from myelocytes in the bone marrow (**Figure 1-2**). Matured neutrophils are released into the blood and circulate throughout an organism's organs and tissues [8]. A mutation or translocation of the genome to prevent myeloid differentiation causes myelodysplastic syndrome or acute myeloid leukemia[9]. The first-choice treatment for AML patients is transplantation. However, all-trans retinoic acid (ATRA) and arsenic trioxide are expected to be useful for induction therapy because they induce myeloid differentiation and stop cellular proliferation. However, these treatments are insufficient to maintain remission. Therefore, it is important to understand the molecular mechanism underlying myelopoiesis and to develop chemotherapies for AML. Acute myeloid leukemia HL-60 cells are a commonly used cell line for modeling of myeloid differentiation [10].

1.1.3. Neutrophil function

Neutrophils directly kill pathogens directly. The primary function of neutrophils is phagocytosis, whereby pathogens are engulfed and degraded by oxygen-dependent and -independent mechanisms. (**Figure 1-3**)[11]. Phagocytosis is initiated by Fcγ receptors, complement receptors, and mannose receptors[12]. IgG-dependent phagocytosis occurs in collaboration with adaptive immunity. In addition, neutrophils secrete Myeloperoxidase (MPO) and alpha-defensin family peptides. Myeloperoxidase produces reactive oxygen species (ROS). Alpha-defensin is highly conserved in mammals and is thought to disrupt microorganisms or host cell membranes by an oxygen-independent mechanism [13].

Neutrophils also express the inflammatory cytokines[14]. IL-1β promotes the production of prostaglandin E_2 and activates neutrophils and lymphocytes. IL-6 promotes the promotion of lymphoid differentiation. IL-8 (and termed CXCL8) is a chemokine that

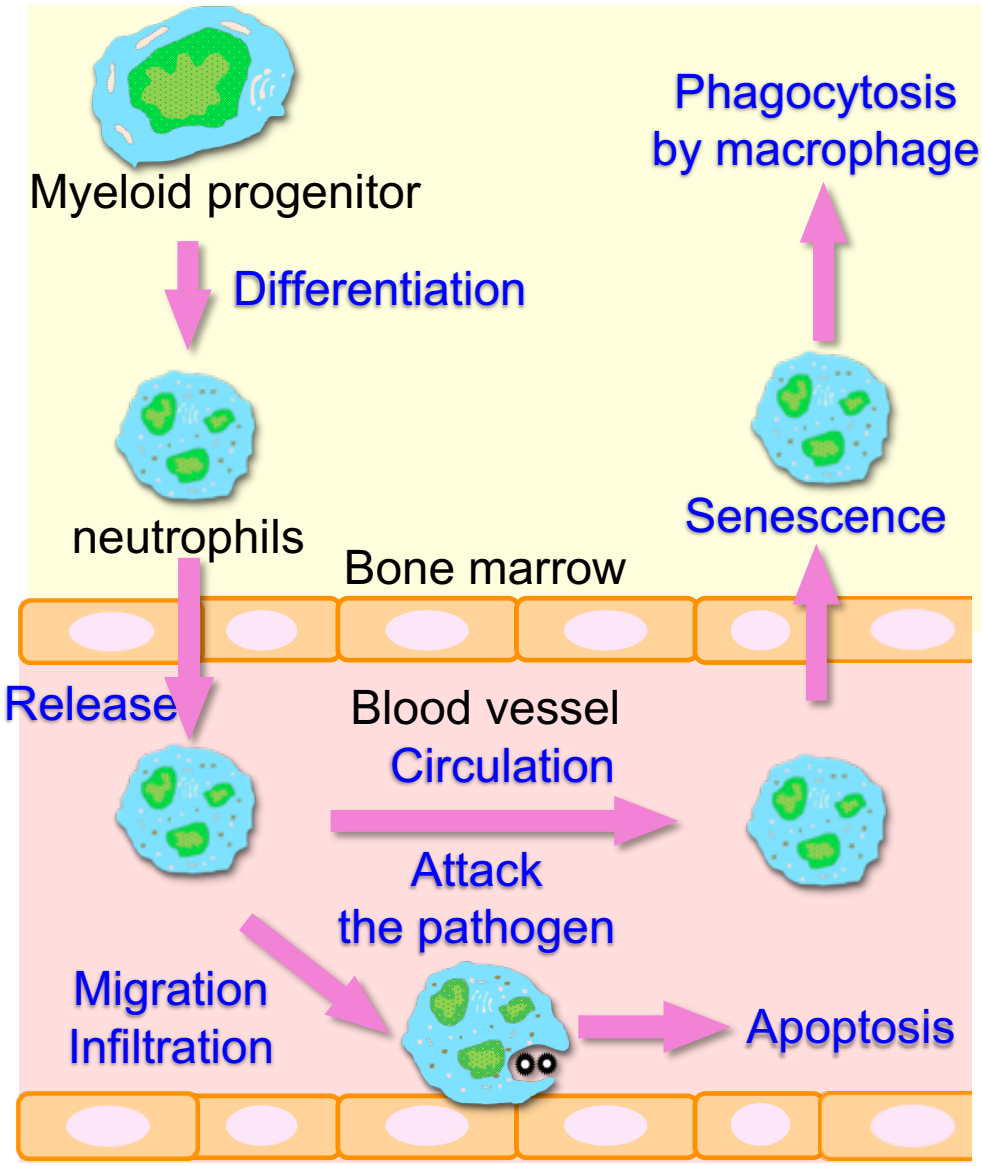

Figure 1-2 Myeloid differentiation

Neutrophils are differentiated from myeloid progenitor, also termed myelocyte, in bone marrow. When they are matured, they are released into blood and circulating. Neutrophils migrate into sites of infection and activate. Activated neutrophils caused apoptosis.

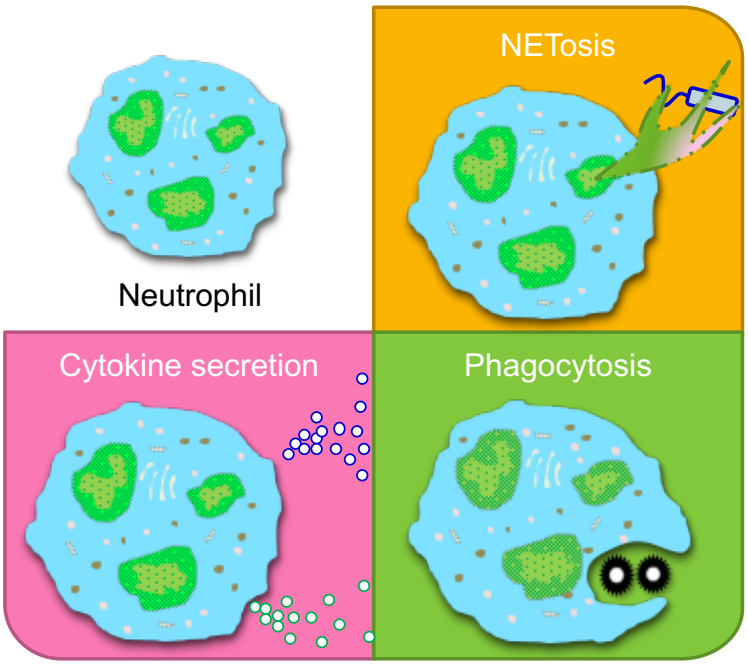

Figure 1-3 Neutrophils functions

Neutrophils, also termed Polymorphonuclear neutrophils, have segmented nucleus. Neutrophils attacked pathogens not only by cytokine secretion but also NETosis and phagocytosis.

induces the neutrophil migration into sites of inflammation. TNF-α regulates fever and apoptosis, inhibits tumorigenesis and viral replication, and is associated with various diseases. Neutrophils contain lipid droplets (also termed lipid bodies) that produce lipid mediators, and these lipid droplets accumulate in leukocytes under inflammatory conditions [15−17]. Nose *et al*. (2013) reported that perilipin-3 was involved in lipid droplet formation, and PGE_2 production, and secretion [18].

1.1.4. Neutrophils heterogeneity and Immune response against cancer

Whether neutrophils affect tumors is controversial [19−21]. Recently, neutrophils were thought to not be a homogeneous population, but rather contain subsets with different characteristics and functions (**Table 1-1**)[22]. One subset is PMN-MDSC, which inhibit immunologically activated states in the late stage of the acute inflammation. However, PMN-MDSC also promotes chronic inflammation, for example in relation to tumors, sepsis, trauma, autoimmune diseases, and transplantation[23−25]. This subset may be similar to low-density neutrophils, tumor-associated neutrophils, and N2-type subsets[26−28]. It is essential to clarify the function of PMN-MDSC to improve their therapeutic use. Furthermore, the mechanisms required to polarize neutrophils towards these subsets are poorly understood.

Cancer immunotherapy is mediated by T cells. Immune checkpoint blockade against PD-1 and CTLA-4 activates CD8 T cells[29]. Chimeric antigen receptor (CAR) T cells are genetically engineered to express an artificial receptor for a cancer-specific antigen[30]. Neutrophils are the most abundant leukocyte, but how neutrophils affect immunotherapy remains unclear. Recently, Ponzetta *et al*. demonstrated that neutrophils mediated resistance against primary carcinogenesis and anti-tumor resistance by neutrophils was dependent on IFN- γ production by T cells [31].

PMN-MDSCs in *Fatp2* knockout mice had abrogated immunosuppressive activity

Table 1-1 Neutrophil heterogeneity

Subset	Function
Low-density neutrophil	↓Phagocytosis, ↑NETosis, ↑IFN, TNF production
PMN-MDSC†	↓Phagocytosis, ↑Inflammation, ↑Immunosuppressive activity
Aged	↑Phagocytosis, ↑NETosis
OLFM4^{+}	↓Cathepsin C activity
TCR^{+}	↑IL-8 production
Angiogenic	↑angiogenesis
CD63^{+}	↓GSH activity ↓Elastase activity
CD49^{+}	Macrophage activation
IL-17^{+}	↑ROS, ↑anti-bacterial activity

(Modified from Silvestre-Roig C. *et al.*, *Blood*, **127**, 2173-2181 (2016)[32])

†Poly Morphonuclear Neutrophil-Myeloid-Derived Suppressor Cell

and these mice had strongly suppressed tumor growth in the T cell-dependent manner [33]. These findings suggest that PMN-MDSC are part of a dominant pathways whereby tumors suppress the immune system. Therefore, it is critical to control the polarization of neutrophils into a suppressive subtype.

1.2. Dephosphorylation

1.2.1. Protein phosphatase

The post-translational modification of proteins is an essential and common mechanism that regulates their functions. Protein phosphorylation, which is highly conserved mechanism, add a functional group on a hydroxyl group and changes the overall charge to negative, Historically, Levene identified a phosphate salt in proteins in 1906[34]. In 1955, Edwin Krebs and Edmond Fischer demonstrated reversible protein phosphorylation by found protein phosphatase. To date, at least 250,000 papers related to protein phosphorylation have been published [35].

In eukaryotes, protein kinases phosphorylate serine, threonine, and tyrosine residues. Kinases and phosphatases can be characterized into two types by their target residues: i) Ser and Thr kinase/phosphatase and ii) Tyr kinase/phosphatase. pSer and pThr account for more than 98% of all phospho-residues in humans [36]. Ser/Thr phosphatases can be classified into three groups, PPP, PPM, and HAD, on the basis of their primary structure and catalytic mechanism. The PPM family contains metal-dependent protein phosphatases with bound Mg^{2+} or Mn^{2+}. Mammals have 20 PPM isoforms, however, substrates of PPM family of phosphatases are poorly understood (**Figure 1-4**)[37].

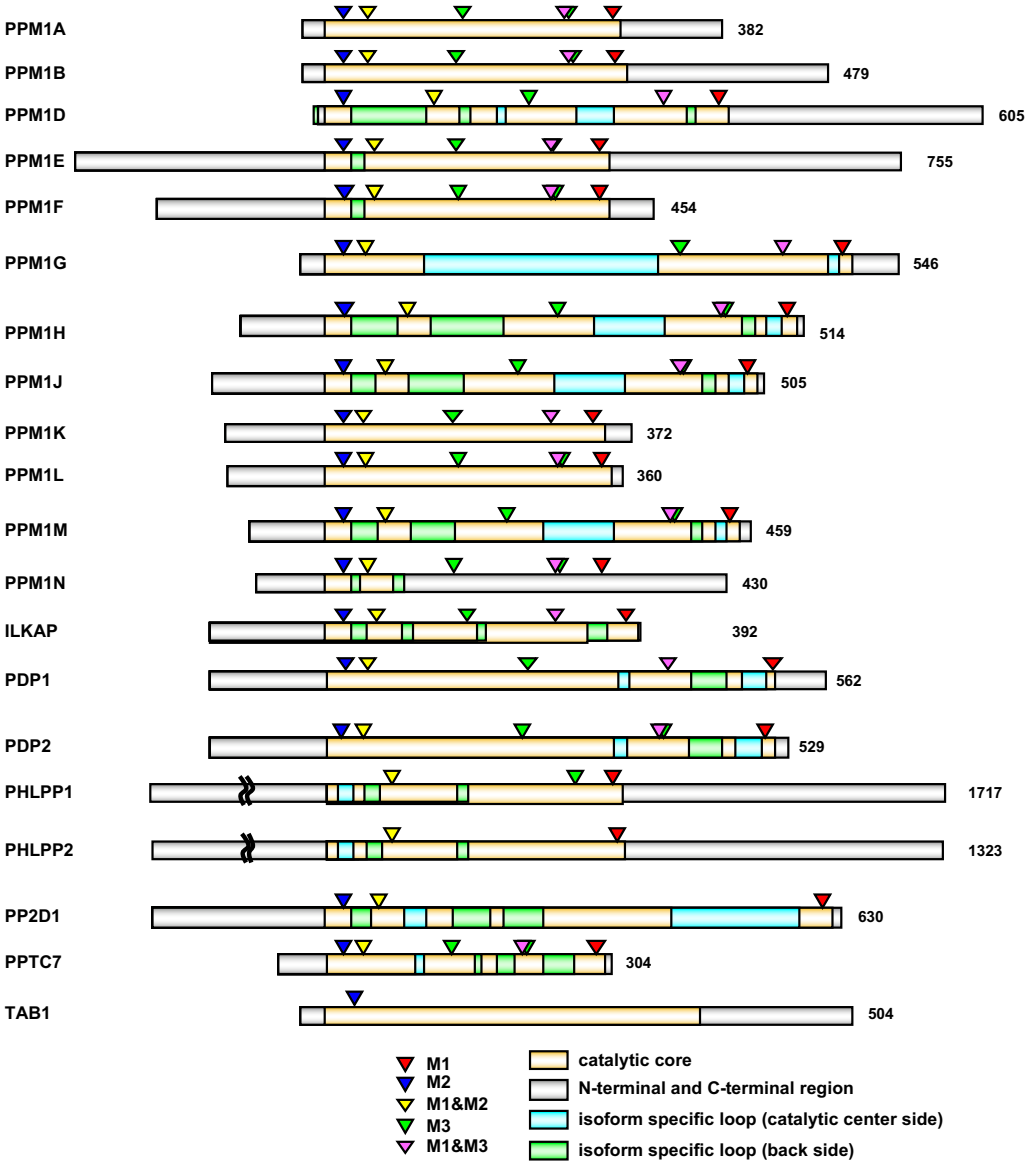

Figure 1-4 PPM family phosphatases

Described domain structures of PPM1 family phosphatases. Their catalytic domains are structurally conserved, indicated in yellow color. And their metal chelating residues are indicated by arrowhead. Loop like inserts on catalytic domains can be divided into two groups: face on catalytic center side or back side.

1.2.2. Ser/Thr phosphatase PPM1D

PPM1D was identified by Dr. Appella's group in 1997 and was reported as a Wild-type p53 inducible phosphatase 1 (Wip1) (**Figure 1-5**) [38]. The *PPM1D* gene maps to 17q23.2. Our laboratory found that PPM1D was alternatively spliced into two variants that have different C-terminal regulatory regions. PPM1D605 is expressed ubiquitously throughout organisms whereas PPM1D430 is specifically expressed in leukocytes and the testis [39].

PPM1D is a negative regulator of the p53 pathway during genotoxic stress responses (**Figure 1-6**). The abnormal hyperactivation of PPM1D was found in several types of tumors[40] and was caused by PPM1D gene amplification, mRNA/protein overexpression, and/or stabilizing mutation. Mutations are important for on clonal hematopoiesis [41] and therapy-related MDS [42]. Thus, PPM1D is considered as a proto-oncogene and a promising drug target for cancer therapies. Several groups have reported a PPM1D-specific inhibitor[43]. Furthermore, we have developed a small molecule inhibitors of PPM1D, SPI-001 and SL-176 (**Figure 1-7**)[44,45]. SL-176 inhibited the proliferation in PPM1D overexpressing cell but not in PPM1D expressing cell at a normal level, indicating SL-176 is a potent small-molecule inhibitor.

The functions of PPM1D in healthy cells have attracted significant attention. In the DNA damage response pathway, PPM1D also dephosphorylates and inactivates ATM, H2AX, and Chk1/2 to promote cell cycle progression [46,47]. Dr. Loewer's group reported that PPM1D expression levels before stress decided the threshold for p53 activation against DNA damage[48]. However, transcriptional regulators of PPM1D except for p53 are currently unknown.

Dr. Donehower's group reported that *Ppm1d* knock out mice had abnormalities including increased inflammation, null T- and B -cell responses, and reduced longevity in male mice[49]. Zhao's group reported that *Ppm1d* knock out mice had neutrophilia

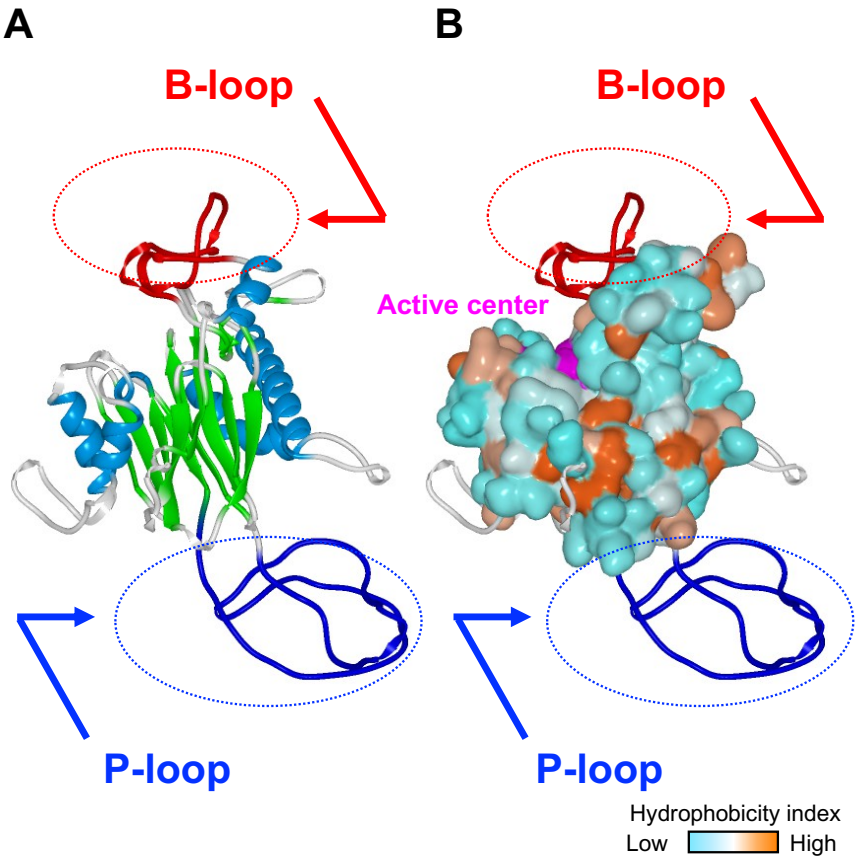

Figure 1-5 Model structure of Ser/Thr phosphatase PPM1D

PPM1D has two unique inserts on catalytic domain: P-loop is Pro-rich long loop which faced on back side and B-loop is Basic amino acid rich loop which faces on same side catalytic center. This homology model was calculated by Modeller 9.11. These templates are PPM1A (4RA2), PPM1B (2P8E), and PPM1K (4DA1).

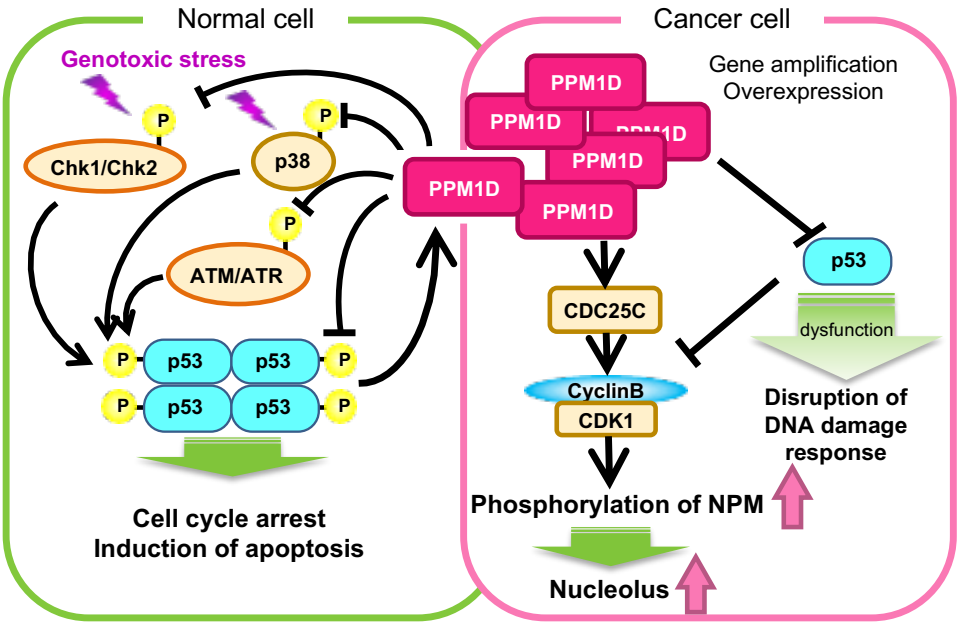

Figure 1-6　The function of PPM1D in DNA damage response pathway

PPM1D is a negative regulator of p53 pathway during DNA damage responses. Our group reported that PPM1D overexpressing cells has many nucleolus［50］.

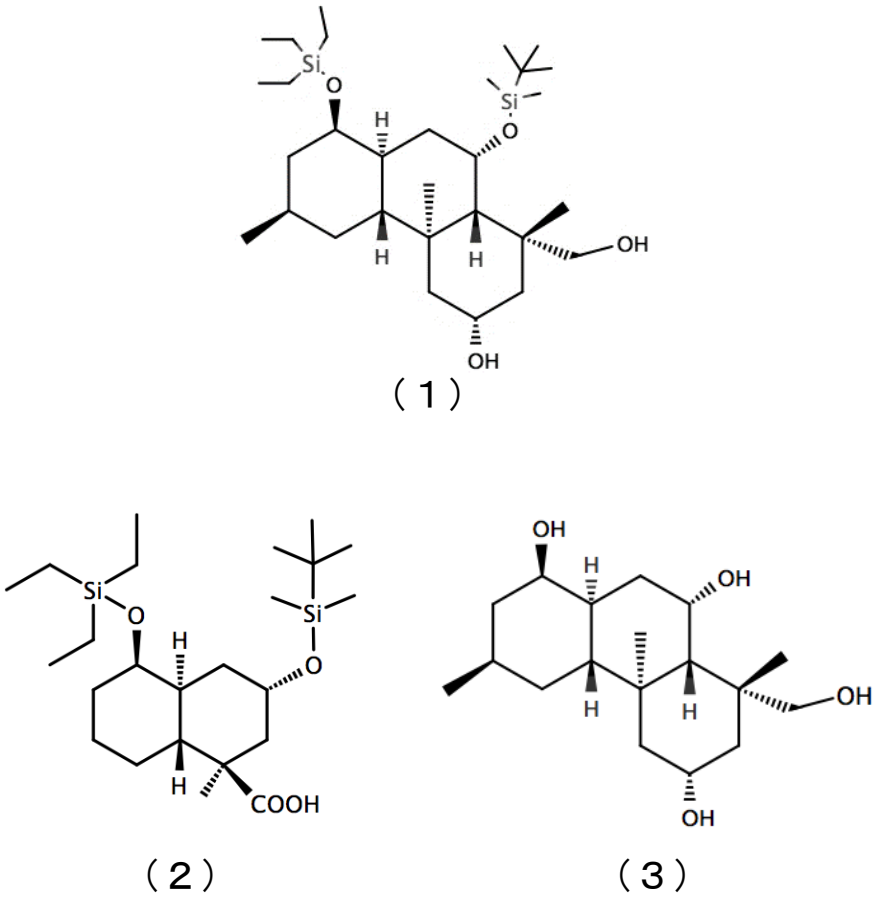

Figure 1-7 Structure of PPM1D inhibitors

Original structure SPI-001 is shown in (1). By structure-function relationship analysis, we developed down-sized and strong inhibitor SL-176, shown in (2). (3) shows inactive analog SL-104.

(an increase in neutrophil numbers) and enhanced inflammation［51］. In addition, our finding regarding alternative splicing suggested that PPM1Ds has specific roles in leukocytes and the testis (**Figure 1-9**). Furthermore, we reported that PPM1D has a vital role in maintaining an undifferentiated state by ERK［52］. We also reported that PPM1D positively regulated lipid droplet formation in adipocytes and is a promising anti-obesity drug target［53］.

1.3. Aim of this study

The molecular mechanism of myeloid differentiation, maturation, and polarization into neutrophil subsets is an important problem for the establishment of more effective therapies for leukemia, chronic inflammation, and tumors. PPM1D is thought to regulate myeloid differentiation and maturation. This study investigated the novel function of PPM1D related to myeloid differentiation using the pharmacological methods.

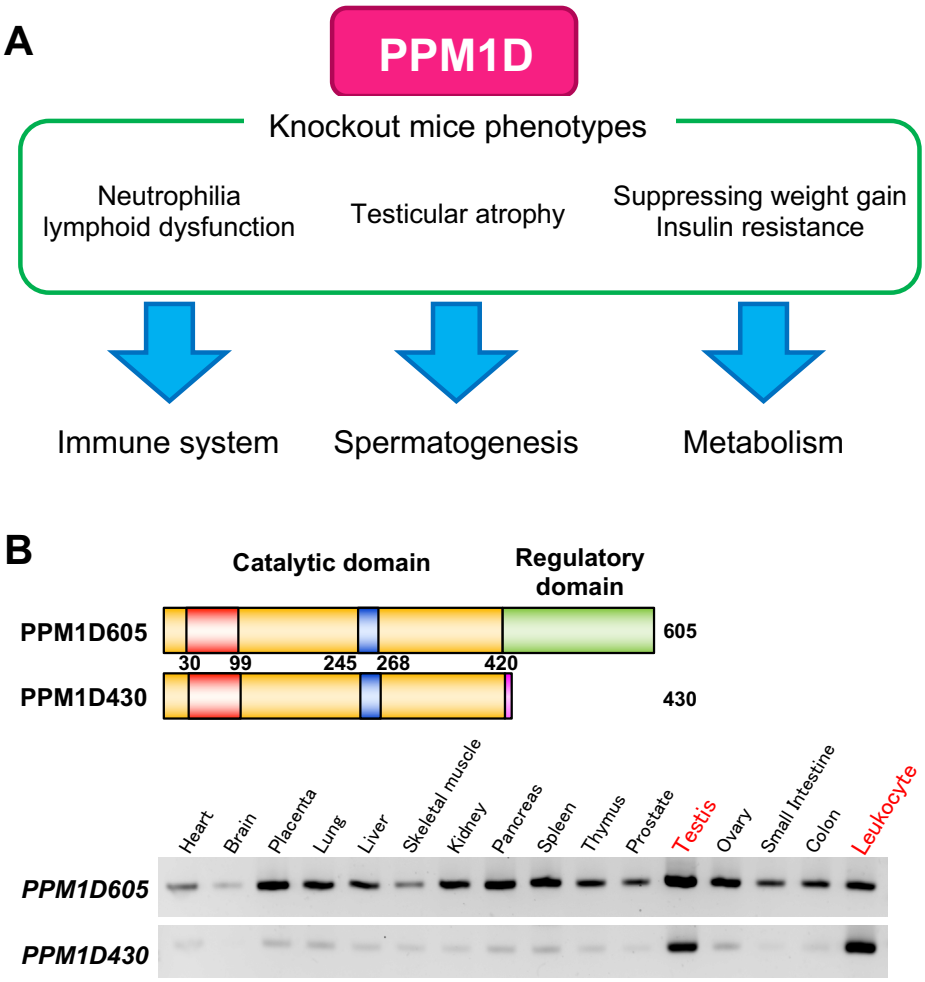

Figure 1-8　PPM1D functions in normal cells

A) *Ppm1d* knockout mice have abnormalities in developments. This suggested PPM1D has important roles in normal tissues. B) Our group reported that PPM1D has two splice variants.

2. Differentiation induction by the pharmacological inhibition of protein phosphatase PPM1D in an acute myeloid cell line HL-60

2.1. Abstract

Protein Phosphatase Magnesium-dependent 1, Delta (PPM1D) is a wild-type p53-inducible Ser/Thr phosphatase that acts as a negative feedback regulator of the p53 tumor suppressor. Gene amplification, overexpression, and gain-of-function mutation of PPM1D have been reported in various cancers, including leukemia. Choi *et al*. reported that *Ppm1d* knockout mice exhibited neutrophilia in the peripheral blood and induced a weak immune response. Previously, I demonstrated that PPM1D inhibition induced myeloid differentiation and G1/G0 cell cycle arrest.

Regarding ATRA treatment, HL-60 increased PPM1D expression during myeloid differentiation. At the same time, the subcellular localization of PPM1D changed from the nucleus to the whole cell including the cytosol. Interestingly, a leukocyte specific variant PPM1D430 had different effects compared with total PPM1D. Furthermore, the inhibition of PPM1D induced neutrophil differentiation from the human acute myeloid leukemia cell line HL-60. Moreover, a novel method to determine the differentiation state was established by using a fluorescent probe TAP-4PH, which has low toxicity, easily stains live cells, and is rapidly removed. The TAP-4PH assay revealed that SL-176 changed the nuclear morphology of HL-60 cells similar to ATRA treated cells. Furthermore, the surface protein and NBT reduction test showed that PPM1D inhibition increased neutrophil-like HL-60 cells. These results suggest that PPM1D inhibition promotes myeloid differentiation. Cell cycle analysis demonstrated that PPM1D inhibition repressed S phase cells. Our group demonstrated that PPM1D inhibition specifically killed PPM1D overexpressing cells. However, HL-60 expressed PPM1D at a basal level. Therefore, this arrest effect was caused by the induction of differentiation.

2.2. Introduction

Neutrophils are the most abundant leukocytes in peripheral blood and form the basis of innate immunity. They are differentiated from myelocytes in the bone marrow and released into the blood. Circulating neutrophils migrate into sites of infection and promote inflammation [11]. Mutations in myelocytic leukemia repress the differentiation and accumulation of myeloblasts, which causes severe immunodeficiencies such as myelodysplastic syndrome and leukemogenesis [54]. Therefore, it is crucial to clarify the molecular mechanism of myeloid differentiation.

Fisciela *et al.* identified Ser/Thr phosphatase PPM1D as a wild-type p53 inducible phosphatase response to ionizing radiation [38]. To date, the abnormal upregulation of PPM1D was found in several types of tumors. This suggested that the hyperactivation of PPM1D inactivates the p53 pathway and promotes tumorigenesis. In the context of clonal hematopoiesis, PPM1D mutation is a hot topic [55,56]. PPM1D stabilization by a truncated mutation in the C-terminal region was found in therapy-related hematologic diseases [57]. PPM1D truncation conferred chemotherapy resistance, leading to the clonal hematopoiesis of mutant cells and PPM1D inhibition reversed the chemotherapy-resistance [58]. Therefore, many groups have investigated PPM1D inhibitors [43]. Our group also developed PPM1D specific inhibitors, SPI-001 and SL-176 [44,45].

Previous reports have focused on negative regulators of the p53 pathway. Dr. Appella's group reported that *Ppm1d* deficient mice exhibited defective T cell and B cell development [38]. However, Zhao *et al.* reported that *Ppm1d* KO mice showed neutrophilia[51]. Also, *Ppm1d* deletion resulted in age-associated phenotypes in HSC such as increase of myeloid-biased HSCs[59]. Furthermore, PPM1D is thought to have a novel function in hematopoiesis.

HL-60 is an acute myeloid leukemia cell line, with p53-null status. HL-60 can acquire a neutrophil-like phenotype by treatment with all-trans retinoic acid (ATRA)[60].

In addition, treatment with phorbol-12-myristate-13-acetate (PMA) changed HL-60 morphology to macrophage-like adherent cells with axons［61］. Although HL-60 do not undergo chromosome translocation, they can differentiate into neutrophils, and are widely used as a model for investigating neutrophil differentiation and functions.

This study analyzed changes in the differentiation state of myeloid cells by PPM1D inhibition and showed that PPM1D inhibition resulted in myeloid differentiation and cell cycle arrest.

2.3. Experimental procedures

2.3.1. Cell culture and induction of differentiation to neutrophil-like cells

HL-60 cells obtained from the American Type Culture Collection (Manassas, VA, USA) were cultured at 37 degree in a 5% CO_2 incubator in RPMI 1640 medium (Sigma-Aldrich, St. Louis, MO, USA) supplemented with 10% (v/v) heat-inactivated fetal bovine serum (FBS), 100 U/mL penicillin and 100 μg/mL streptomycin (ThermoFisher SCIENTIFIC, CA, USA). HL-60 cells were induced to differentiation by the treatment of various agents to cell culture a day after seeding: 1 μM ATRA (Sigma-Aldrich, St. Louis, MO, USA), 7.5 μM PPM1D-specific inhibitor SL-176 and 7.5 μM Sl-104, an inactive inhibitor of PPM1D. And then, added 200 μL of media containing agent every 2 days.

2.3.2. Quantitative Real-time PCR

For RNA preparation, HL-60 cells were harvested by TRIzol reagent (ThermoFisher SCIENTIFC), and then total RNA on each sample were purified according to manufacturer's protocol. Purified RNA was reverse transcription by using PrimeScript II 1st strand cDNA Synthesis Kit (Takara, Kyoto Japan) with random hexamer primer according to manufacturer's instruction. For quantitative PCR, I used iTaq Universal SYBR Green Supermix (Bio-rad, CA, USA). And used primer sequences were described in **Table 2-1**. I used CFX96 Touch real-time PCR detection system (Bio-rad). In this thesis, all results were shown as a relative expression against Hypoxanthine-guanine phospho- ribosyltransferase (HPRT) to normalize a loading cDNA amount. The expression was calculated by the Ct method.

Table 2-1 Primer list used in Chapter 2

Primer	Sequence
C/EBPE-forward	CCACGGGACCTACTACGAGT
C/EBPE-reverse	ACGGCAAAGAGATCGGAGAGA
PPM1D605-forward	ACCAGTCAAGTCACTGGAGG
PPM1D605-reverse	ATTGCTACGAACCAGGGCAG
PPM1D430-forward	CCACCAGTCAAGGATTTTGGA
PPM1D430-reverse	TACACATGGCTGGCATTCAGA
HPRT-forward	CCTGGCGTCGTGATTAGTGAT
HPRT-reverse	AGACGTTCAGTCCTGTCCATAA

2.3.3. Western Blotting

HL-60 cells were transferred into tubes. Aliquots were spun down for 5 min at 700xg. The pellets were suspended in PBS. They were spun down again and were suspended in 75 μL of 1x sample buffer (50 mM Tris-HCl, pH 6.8, 2% sodium dodecyl sulfate, 6%(v/v) 2-mercaptoethanol, and 10% glycerol). Their samples were separated by 10% SDS-PAGE and then transferred to a PVD membrane. Immunoblotting was performed with the antibodies, primary; rabbit polyclonal anti-PPM1D and GAPDH, and then the membranes were incubated with secondary; anti-rabbit IgG-HRP. Protein were detected by enhanced chemiluminescence with the following antibodies.

2.3.4. Immunofluorescence

The HL-60 cells were harvested and fixed 15 min by 3.7% formaldehyde. They were washed with PBS containing 2% FBS, permeabilized with 70% ice-cold methanol/PBS at -20 degree for 15 min and blocked with 10% FBS/PBS for 1 hour. The cells were then incubated for overnight with a primary rabbit polyclonal anti-PPM1D antibody, followed by 1-hour incubation with a secondary antibody, AlexaFluor 568 goat anti-rabbit IgG (Molecular probe). The cells were stained with DAPI for the counterstain and observed by fluorescence microscopy (Biorevo BZ-9000, KEYENCE, Osaka, Japan).

2.3.5. Counting the cell with lobed and segmented nuclei

For the visualization of nuclear morphology, I used the fluorescent probe TAP-4PH, 1, 3a, 6a-triazapentalene derivative. Cells were collected and treated with TAP-4PH (Final concentration: 50 μM in 2% FBS/PBS). The cells were incubated at 37 degree for 30 minutes, and then observed under the fluorescence microscopy using the DAPI-B (Ex360/40, Dm400, Em460/50) filter. The numbers of neutrophils with lobed and segmented nuclei were counted manually.

2.3.6. Flow cytometry analysis

The cells were harvested, washed by PBS containing 2% FBS, and then labeled using the Live/Dead Fixable Dead Cell Stain Kit (ThermoFisher SCIENTIFIC, CA, USA) according to manufacturer's protocol for gating live cells. The cells were washed, incubated with Human TruStain FcX (Biolegend, San Diego, CA, USA) for 10 minutes to block IgG-involved unwanted staining. Besides, they were washed and incubated with an antibody against CD11b/MAC-1 (FITC Mouse anti-Human CD11b/MAC-1, BD Bioscience, San Jose, CA, USA) for 30 minutes. After washing again, they were fixed with 3.7% formaldehyde and stored with 70% ice-cold methanol. Fluorescent analysis was performed by flow cytometer. Data were analyzed by FlowJo software.

2.3.7. Cell cycle analysis

The cells were harvested, fixed by 70%-ice cold ethanol and incubated at -20 degree for 15 minutes at least. After washing out ethanol, they were stained by PI/RNase buffer (BD Pharmingen, San Diego, CA, USA). Cellular DNA content was measured by flow cytometer. Data were analyzed by FlowJo software.

2.4. Results

2.4.1. PPM1D expression profiles during differentiation

The PPM1D expression pattern in HL-60 was analyzed before and after differentiation. ATRA was added into HL-60 culture media for 2, 4 and 6 days. ATRA is known as a neutrophil inducer for acute myeloid cell lines, including HL-60. The mRNA expression level of PPM1D was analyzed. During myeloid differentiation, transcriptional factor CEBPE, a terminal differentiation marker in myelocytes, was increased by ATRA treatment ［62］. Similar to previous studies, *CEBPE* expression levels were increased in HL-60 (**Figure 2-1**).

PPM1D is considered a p53-inducible gene and a negative feedback regulator in the p53 pathway. HL-60 does not express p53. During the differentiation of HL-60 cells, PPM1D mRNA and protein expressions were also increased during differentiation (**Figure 2-1, 2-2**). A comprehensive analysis using the Chip-seq database online was performed and a protein binding cluster region nearby PPM1D Exon 1 and at least 100 transcriptional factors lacking p53, which bound to that region were identified (**List 2-1**). This suggested that PPM1D expression in HL-60 is induced by a p53-independent mechanism.

PPM1D was reported to be localized in the nucleus ［39］. Furthermore, its substrates, p53, p38, ERK, and Chk1/2, were also localized in the nucleus. The subcellular localization of PPM1D was analyzed by immunocytochemistry. PPM1D in undifferentiated HL-60 was localized to the nucleus, especially the nucleolus (**Figure 2-3A**). After ATRA treatment, differentiated cells with a banded or segmented nucleus were observed. PPM1D was also localized to the cytosol in ATRA-differentiated HL-60 cells, which had lobbed nuclei. Interestingly, a PPM1D430 specific antibody used to visualized PPM1D demonstrated cell nuclei lacking a nucleolus and cytosol.

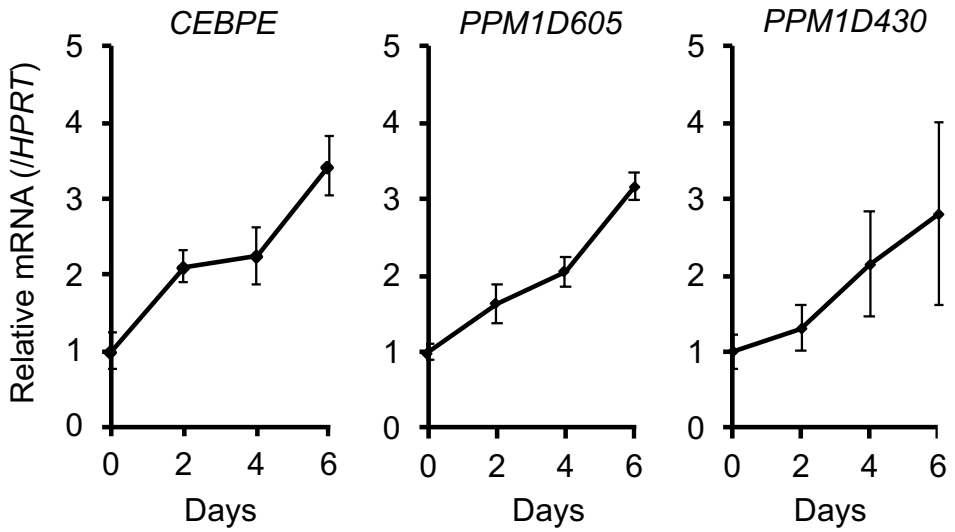

Figure 2-1 mRNA expression profile during myeloid differentiation

HL-60 cells were treated with 1 μM ATRA for 2, 4, 6 days, and then mRNA levels, C/EBPE, PPM1D605, PPM1D430 and HPRT were quantitatively analyzed by RT-PCR, normalized to HPRT mRNA expression. Each y-axis indicate expression as fold of 0 day.

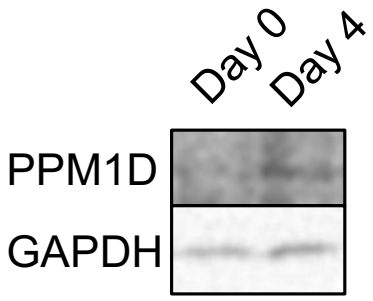

Figure 2-2　Expression level of PPM1D in HL-60

Before treatment control (Day 0) and ATRA-treated HL-60 cells for 4 days were harvested. Final concentration of ATRA was 1 μM. PPM1D protein was detected by immunoblot analysis. GAPDH was used as a loading control.

List 2-1 List of putative transcriptional regulator of PPM1D in blood by the analysis on Chip-seq database［63］

ARNTL, ATF1, ATF2, BRD4, BRD7, CBFB, CBX3, CCNT2, CDK8, CDK9, CEBPA, CEBPB, CEBPD, CHD1, CHD2, CPSF3L, CREB1, CTCF, CTCFL, DPF2, E2F4, E2F6, EGR1, ELF1, EP300, ERG, ETS1, FLI1, FOS, GABPA, GATA1, GATA2, HCFC1, HDAC1, HDAC2, HEY1, HMGN3, ILF3, INTS13, IRF1, JMJD1C, JUN, JUND, KDM1A, KDM2B, KDM5B, KMT2A, LDB1, LMO2, LMO3, MAX, MAZ, MEF2C, MLLT1, MYC, MYH11, NFYA, NFYB, NR2F2, NR3C1, NR4A1, NRF1, PHF8, PLAG1, PML, RAD21, RBBP5, RCOR1, REST, RFX5, RUNX1, RUNX1T1, SAP30, SIN3A, SKI, SMAD1, SMARCA4, SMC1A, SP2, SPI1, STAG1, STAT1, SUMO2, SUPT5H, TAF1, TAF7, TAL1, TBP, TCF3, TEAD4, TRIM24, TRIM28, TRP47, UBTF, YY1, ZBTB33, ZBTB7A, ZFP64, ZNF143, ZNF263

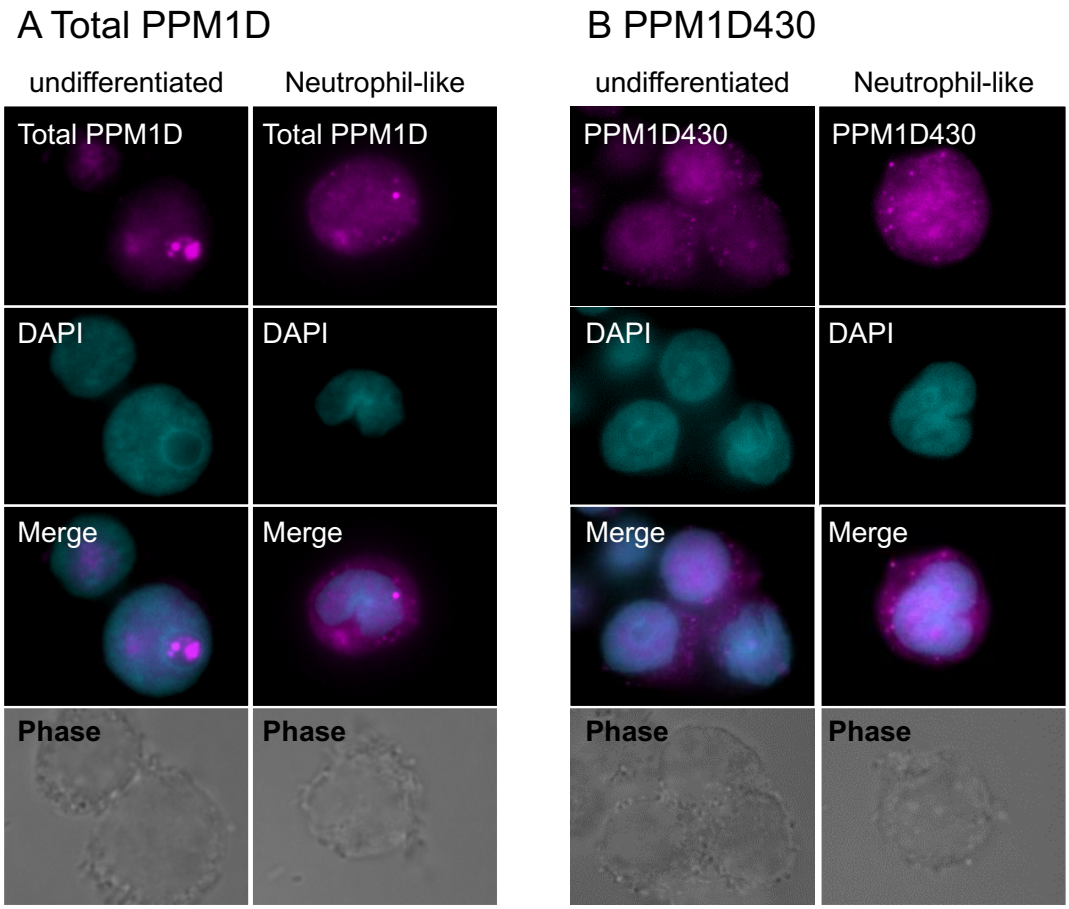

Figure 2-3 Subcellular localization of PPM1D in HL-60

(A) Untreated control (undifferentiated) and 1 μM ATRA-treated cells for 6 days were fixed and stained with the antibody which epitope is in common region in N-terminal catalytic domain (B) antibody recognized PPM1D430. Neutrophil-like cells were decided by nuclear shapes.

These results suggest that PPM1D regulation was different before and after differentiation, and that PPM1D dephosphorylated different targets. Furthermore, I revealed that PPM1D430 and PPM1D605 were localized to different regions in cells.

2.4.2. PPM1D inhibition induces morphological changes, and TAP-4PH can visualize the nuclear shape in HL-60.

SL-176 is a PPM1D-specific inhibitor that was developed in collaboration with the Laboratory of Organic Chemistry II. PPM1D inhibition of HL-60 cells was performed to study its effects on morphology. HL-60 morphology was analyzed by a novel fluorescent probe TAP-4PH, a 1, 3a, 6a-triazapentalene derivative. Although TAP-4PH can be used to visualize nuclear segmentation, this low-toxicity and easy-to-use probe that showed high fluorescence in the cytoplasmic area. TAP-4PH can also visualize nuclear segmentation, I used this probe. TAP-4PH demonstrated ATRA-induced HL-60 had lobbed and segmented nuclei. Next, HL-60 were treated with the PPM1D inhibitor SL-176. HL-60 displayed a neutrophil-like morphology, but they are not adherents and had no axon (**Figure 2-4**). This suggests that PPM1D inhibition induced neutrophil differentiation but not monocytic differentiation and that TAP-4PH is a useful compound for differentiation induction. Furthermore, PPM1D inhibition significantly increased the number of neutrophil-like cells (**Figure 2-5, Table 2-2**) and in combination with ATRA, it increased the efficiency of differentiation compared with single treatment. In contrast, an inactive PPM1D inhibitor analog SL-104 did not show to induce the differentiation.

2.4.3. PPM1D inhibition induces myeloid differentiation into neutrophils.

Analysis of the expression of surface differentiation marker CD11b on single neutrophils was performed [64]. PPM1D inhibition increased the number of $CD11b^{+}$ cells whereas the inactive analog SL-104 had no effect (**Figure 2-6**). A combination of

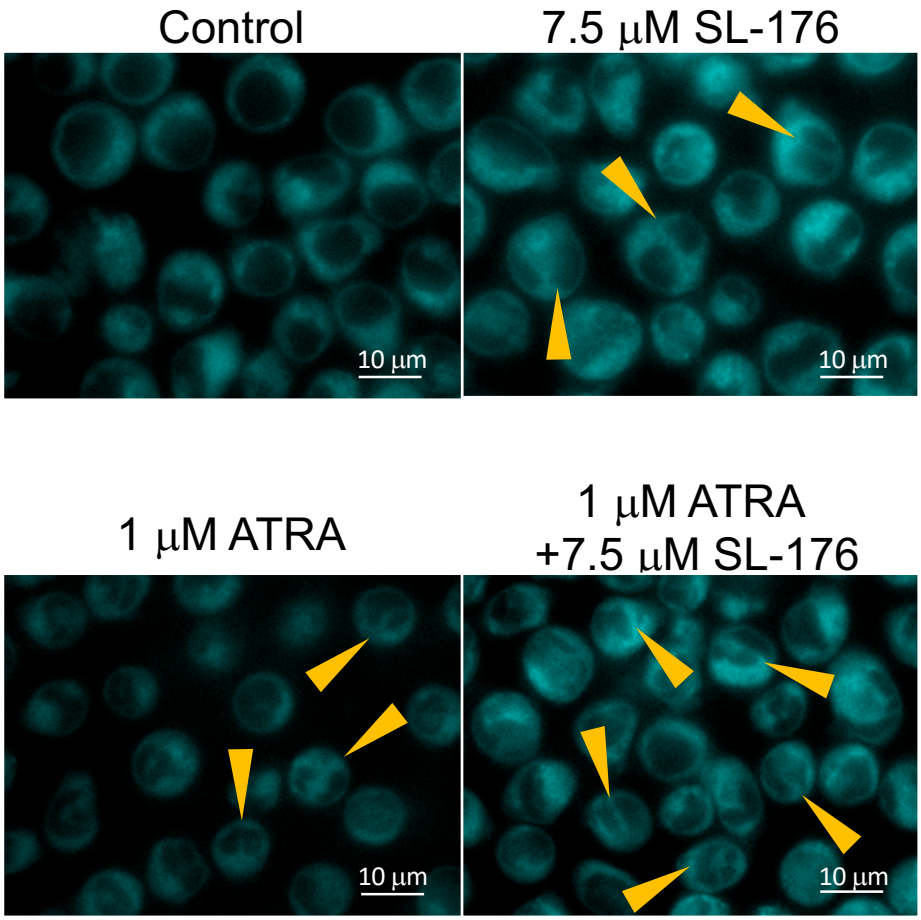

Figure 2-4 TAP-4PH staining visualized cellular shape and nuclear segmentation.

Each cell treated with the indicated agents (1 μM ATRA and/or 7.5 μM SL-176) for 6 days. The cells were incubated 30 minutes with 50 μM TAP-4PH before obtained.

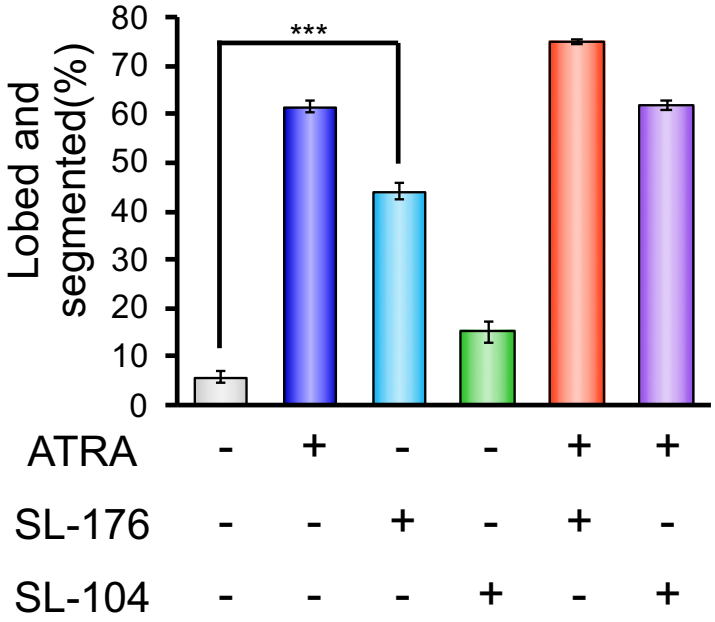

Figure 2-5 PPM1D inhibitor induces the morphological change in HL-60 cells.
Percentages of cells with banded and segmented nuclei among HL-60 cells. Each cell treated with the indicated agents (1 μM ATRA and/or 7.5 μM SL-176) for 6 days. The cells were incubated 30 minutes with 50 μM TAP-4PH before obtained. ***p<0.001

Table 2-2 PPM1D inhibitor induces the morphology of HL-60 cells

Compounds	%differentiated (morphology)
Control	5.8 ±1.3%
ATRA	61.5 ±1.3%
SL-176	44.1 ±1.6%
ATRA + SL-176	74.9 ±0.7%

The percentage of cells with banded and segmented nuclei among HL-60 cells

ATRA and SL-176 increased myeloid differentiation more than ATRA alone, and SL-104 had no effect.

In the clinic, an NBT reduction test is performed to measure the neutrophil count in peripheral blood. PPM1D inhibition also increased NBT reduction activity (**Figure 2-7**). Moreover, differentiated cells were increased with culture time (**Table 2-3**). These results demonstrate that PPM1D inhibition induces myeloid differentiation into neutrophils, and that is combined treatment with ATRA is more efficient than that with ATRA alone.

2.4.4. Cell cycle analysis after PPM1D inhibition

Terminally differentiated neutrophils have an arrested cell cycle [65]. Therefore, cell cycle analysis was performed to reveal whether SL-176 arrested HL-60 cell growth similar to ATRA-treated HL-60 [66]. PI stained HL-60 were measured by flow cytometry (**Figure 2-8, Table 2-4**). SL-176 treatment increased the ratio of G1/G0 cells by 5.9%. Our group previously reported that SL-176 specifically inhibited the proliferation of PPM1D overexpressing cells, but not cells expressing a normal level of PPM1D [45]. In undifferentiated HL-60, the expression of PPM1D protein was not high; thus, cell cycle arrest was caused by the induction of myeloid differentiation.

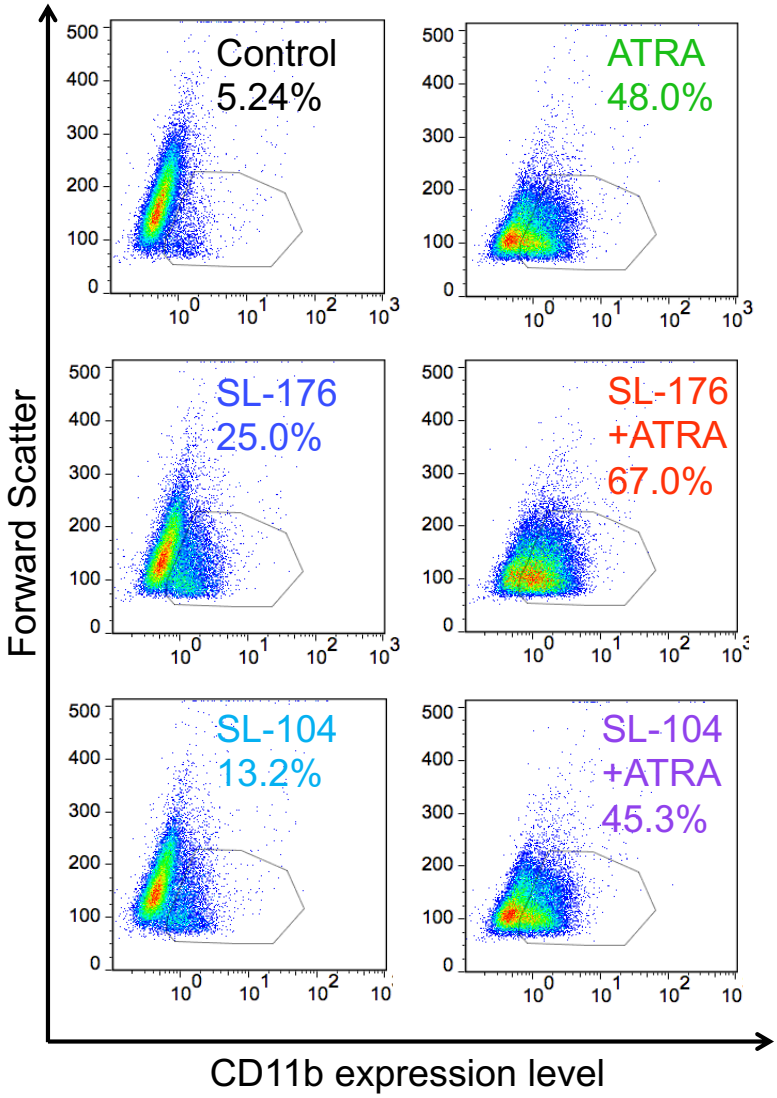

Figure 2-6 The expression of surface marker protein CD11b for myeloid differentiation

Flow cytometric analysis was performed with an anti-CD11b antibody labeled with FITC. HL-60 cells were treated with the indicated agents (1 μM ATRA, 7.5 μM SL-176 and/or 7.5 μM SL-104) for 6 days. Apoptotic cells were removed by gating by forward and side scatter patterns and fluorescence of Live/Dead fixable Dead Cell Stain kit. Gate for CD11b positive cells was decided by comparing with isotype-matched control.

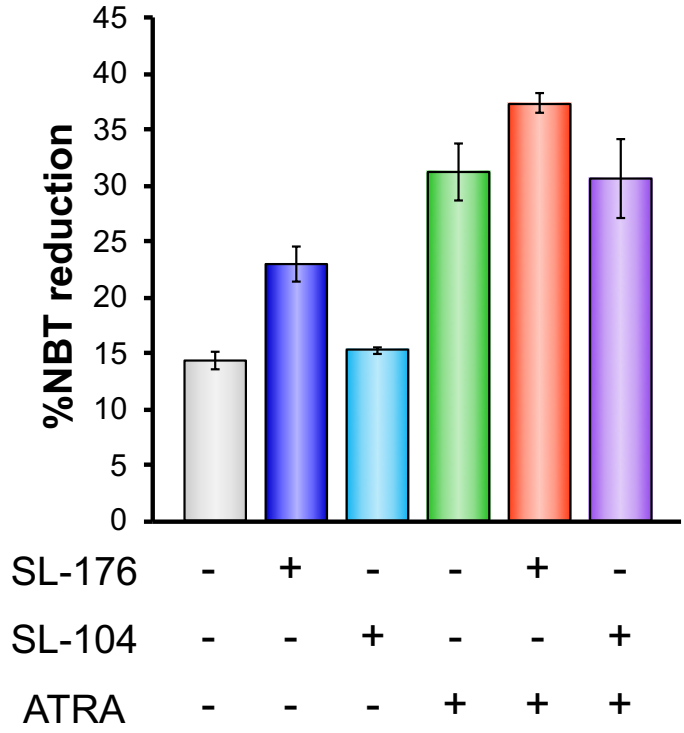

Figure 2-7 PPM1D inhibition increases NBT reduction Positive cells in HL-60 at day 4.

HL-60 cells were treated with the indicated agents (1 μM ATRA, 7.5 μM SL-176, and/or 7.5 μM SL-104) for 4 days and then NBT reduction test was performed. Here is shown the percentage of NBT-positive cells.

Table 2-3 PPM1D inhibitor increased NBT reduction activity in HL-60 cells.

Compounds	%differentiated (NBT reduction test)			
	Day 4		Day 6	
Control	14.3 ±0.8%		14.3 ±0.9%	**
ATRA	31.3 ±2.6%	***	37.8 ±0.9%	
SL-176	23.0 ±1.5%		26.9 ±3.7%	***
ATRA + SL-176	37.4 ±0.9%		51.0 ±0.8%	

The percentage of NBT-positive cells was analyzed manually with a counter. Data represent the mean ± SD of three independent experiments. **p<0.01, ***p<0.001, *t*-test

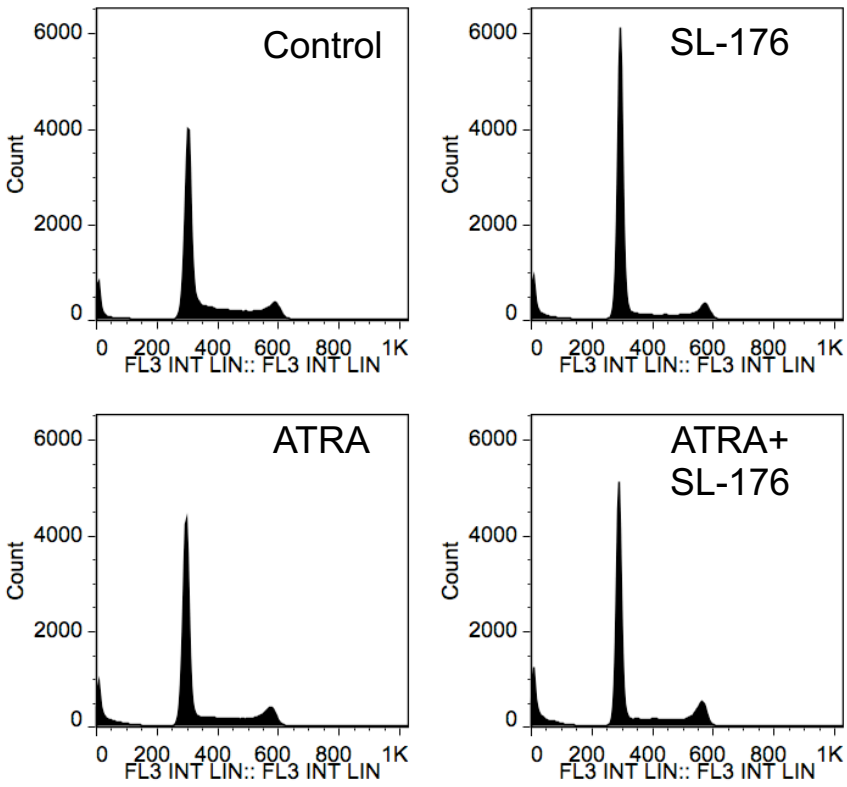

Figure 2-8 Cell cycle analysis of HL-60 cells

HL-60 cells were treated with the agents (1 μM ATRA, 7.5 μM SL-176 and/or 7.5 μM SL-104) for 2 days. The cells were fixed with 70% ethanol and stained with PI/RNase staining buffer. DNA cell cycle analysis was performed by flow cytometry.

Table 2-4 Cell cycle analysis of HL-60 cells

ATRA	-	+	-	-	+	+
SL-176	-	-	+	-	+	-
SL-104	-	-	-	+	-	+
G1/G0	55.7	76.1	61.6	60.2	65.8	70.2
S	34.3	15.8	27.6	29.8	21.1	19.1
G2/M	10.0	8.1	10.8	10.0	13.1	10.8

For the fitting of cell cycle, Watson pragmatic algorithm was used.

2.5. Discussion

The first chapter demonstrated PPM1D was increased during myeloid differentiation. Zhao *et al*. showed that PPM1D expression levels were increased from HSC to mature neutrophils. The current study results are in accordant with this report. Interestingly, the subcellular localization of PPM1D was different between total PPM1D and PPM1D430. Our group found that PPM1D430 lacking a C-terminal domain NLS ^{535}KRTLEESNSGPLMKKHRR^{552} and PPM1D430 localized to the nucleus, cytoplasm and plasma membrane in the T47D cell line. However, PPM1D was localized to the nucleus only in a PPM1D overexpressing breast cancer cell line MCF7. These results suggest that PPM1D localization is regulated in a context-dependent manner.

Next, PPM1D inhibition was performed and the differentiation status was determined. TAP-4PH morphological analysis revealed that PPM1D inhibition induced myeloid differentiation but not macrophage differentiation. Furthermore, it demonstrated that TAP-4PH can be used to visualize the shapes of nuclei and determine the differentiation state. TAP-4PH staining is a rapid method with low cytotoxicity, and it is easily removed from cells. Stained cells can be used for other assays. Our group recently reported that PPM1D has an essential role in the maintenance of the undifferentiated state ［52］. Moreover, Zhao *et al*. reported that *Ppm1d* knockout mice had neutrophilia, the abnormal increase of peripheral neutrophils. Consistent with these reports, these results demonstrated that PPM1D negatively regulates myeloid differentiation into neutrophils (**Figure 2-9**).

Lastly, the effect of the SL-176 on the cell cycle was analyzed. SL-176 increased cell cycle arrest in cells. The HL-60 cell line has a p53-null status and basal PPM1D expression. Therefore, this cell cycle arrest resulted from cellular differentiation. Recently, PPM1D truncated mutations in the C-terminal regulatory region were reported for several tumors. Some PPM1D truncated mutants are hyperstabilized suggesting that

PPM1D truncated mutants promote tumorigenesis by a p53-dependent mechanism. However, PPM1D truncated mutations in therapy-related MDS are not a complete phenocopy of TP53 mutations ［42］. From the current results, PPM1D hyperactivity in clonal hematopoiesis may disrupt the p53 pathway to induce abnormalities in myeloid differentiation. Therefore, PPM1D inhibition is a promising target for chemotherapy against PPM1D mutations in AML and MDS.

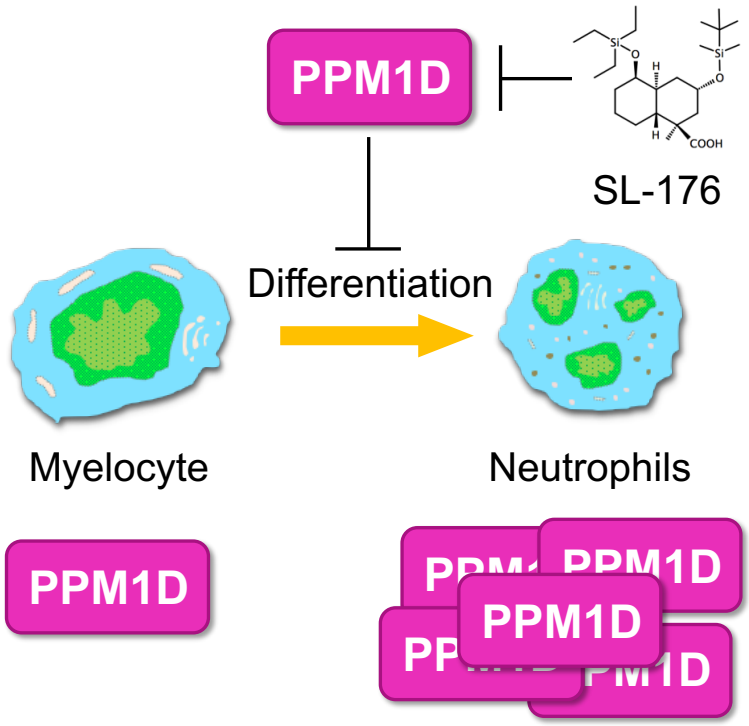

Figure 2-9　PPM1D function in myeloid differentiation

PPM1D may repressed myeloid differentiation into neutrophils, because PPM1D inhibition induced it. On the other hand, PPM1D expression level was increased during differentiation. These results suggest PPM1D has another role and target after differentiation.

3. Immunosuppressive activity of PPM1D inhibited neutrophils

3.1. Abstract

Neutrophils are critical effector cells in the early phase of host defense, and they remove pathogens by engulfing the bacteria via phagocytosis, expressing anti-bacterial molecules, and activating other immune cells by secreting cytokines. Recently, it was reported that neutrophils with different properties can be categorized into subsets. Protein phosphatase PPM1D is a negative regulator of p53 in the DNA damage response pathway. Phenotypic analysis revealed that *Ppm1d* KO mice had abnormal hematopoiesis and neutrophilia. Previously, we reported that PPM1D has two alternative splice variants, ubiquitously expressed PPM1D605 and PPM1D430, which is specifically expressed in leukocytes. This suggested that PPM1D has novel functions in leukocytes. In chapter 2, the function of PPM1D in myelocytes and neutrophils was analyzed using the acute myeloid leukemia cell line HL-60. We developed a PPM1D specific inhibitor, SL-176, which induced the differentiation of HL-60 into neutrophils.

In this chapter, the phagocytotic activity and cytotoxicity of HL-60 were analyzed. The results showed that phagocytotic activity was markedly decreased by PPM1D inhibition. Furthermore, PPM1D-inhibited repressed T cell proliferation in HL-60 and the inhibition of PPM1D catalytic activity repressed HL-60 cytotoxicity against tumor cells. To clarify the mechanism of cell polarization, lipid mediator secretion and lipid body formation in neutrophils were investigated. PPM1D inhibition induced polarization into PMN-MDSC-like cells via the promotion of PGE_2 production.

Next, RNA-seq transcriptome analysis of HL-60 was performed in the presence or absence of SL-176. Interestingly, the addition of SL-176 changed the gene expression profiles, especially those related to phagocytosis or cytotoxicity. Of note, COX-2 and mPGES-1, PGE_2 synthesis cascade genes from arachidonic acid, were increased. Thus,

this study suggested that PPM1D regulates myeloid differentiation and neutrophil functional maturation, and that this is partly caused by a change in the transcriptome. This study is the first report of the essential requirement for protein phosphatases to maintain the functionality of innate myeloid immunity.

3.2. Introduction

Neutrophils are the leukocytes that have import roles in innate immunity. Neutrophils migrate into sites of infection or damaged tissues, engulf targets by phagocytosis, secrete ROS or oxygen-independent molecules, and produce inflammatory cytokines, which help remove the pathogens [67]. Recently, the anti-tumor effects of neutrophils have attracted significant attention [21,68,69], although pro- and anti-tumor effects of neutrophils have been reported [31,33].

Neutrophils are not a uniform cell type and they have heterogeneous functions, especially those polarized into low-density neutrophils, PMN-MDSC, tumor-associated neutrophils, or N2 type neutrophils, which exhibit immunosuppressive activity and pro-tumorigenic phenotypes [22,32]. Veglia F. *et al*. reported that the deletion of immunosuppressive activity in PMN-MDSC strongly repressed tumor growth, which was clearly reversed by neutralizing antibodies against $CD8^+$ T cells [70]. Therefore, it is critical to clarify the molecular mechanism of polarization for the establishment of more effective cancer immunotherapies.

Prostaglandin E_2 is proinflammatory lipid mediator. PGE_2 has a predominant role in tumorigenesis and is the most abundant prostaglandin present in various tumors. PGE_2 induces proliferation by activating Ras-ERK and GSK3b-catenin signals in colon and lung cancer. In this way, PGE_2 canonically promotes tumorigenesis by the inhibition of apoptosis, and enhancement of proliferation and angiogenesis. Interestingly, Prima *et al.* (2017) reported that the COX2/mPGES1/PGE_2 cascade was increased in BM-derived CD11b myeloid cells by tumor cells and that PGE_2 promoted the expression of PD-L1 in myeloid cells [71]. PGE_2 also promoted tumorigenesis via the downregulation of immune myeloid responses and inflammatory responses against tumor.

Protein phosphatase PPM1D was originally considered as just a negative feedback protein in the tumor suppressor p53 pathway against cellular stress. However, the

knockout experiment revealed that PPM1D has other functions including hematopoiesis. Zhao *et al*. reported that *Ppm1d* knockout mice show neutrophilia and increased inflammation. Furthermore, Dr. Appella's group reported that these mice exhibited defective T cell maturation and impaired antigen-independent B-cell development. However, PPM1D has functions in the crosstalk between innate immunity and adaptive immunity.

In this chapter, I analyzed the neutrophils functions of differentiated HL-60, inflammatory response, phagocytosis, T cell proliferation, and cellular cytotoxicity were analyzed. The results showed that PPM1D inhibition induced the polarization into immunosuppressive neutrophils via the enhancement of the COX-2/mPGES-1/PGE_2 cascade and lipid droplet formation.

3.3. Experimental procedures

3.3.1. Cell culture and induction of differentiation to neutrophil-like cells

HL-60, Jurkat and A549 cells obtained from the American Type Culture Collection (Manassas, VA, USA) were cultured at 37 degree in a 5% CO_2 incubator in RPMI 1640 medium (Sigma-Aldrich, St. Louis, MO, USA) supplemented with 10% (v/v) heat-inactivated fetal bovin serum (FBS), 100 U/mL penicillin and 100 μg/mL streptomycin (ThermoFisher SCIENTIFIC, CA, USA). HL-60 cells were induced to differentiation by the treatment of various agents to cell culture a day after seeding: 1 μM ATRA (Sigma-Aldrich, St. Louis, MO, USA) and 7.5 μM PPM1D-specific inhibitor SL-176. And then, added 200 μL of media containing agent every 2 days.

3.3.2. Quantitative Real-time PCR

For RNA preparation, HL-60 cells were harvested by TRIzol reagent (ThermoFisher SCIENTIFC), and then total RNA on each sample were purified according to manufacturer's protocol. Purified RNA was reverse transcription by using PrimeScript II 1st strand cDNA Synthesis Kit (Takara, Kyoto Japan) with random hexamer primer according to manufacturer's instruction. For quantitative PCR, I used iTaq Universal SYBR Green Supermix (Bio-rad, CA, USA). And used primer sequences were described in **Table 3-1**. I used CFX96 Touch real-time PCR detection system (Bio-rad). In this thesis, all results were shown as a relative expression against Hypoxanthine-guanine phospho- ribosyltransferase (HPRT) to normalize a loading cDNA amount. The expression was calculated by the Ct method.

Table 2-1 Primer list used in Chapter 2

Primer	Sequence
IL1B-forward	ATGATGGCTTATTACAGTGGCAA
IL1B-reverse	GTCGGAGATTCGTAGCTGGA
IL6-forward	ACTCACCTCTTCAGAACGAATTG
IL6-reverse	CCATCTTTGGAAGGTTCAGGTTG
IL8-forward	TCTGTGTGAAGGTGCAGTTTTG
IL8-reverse	AATTTCTGTGTTGGCGCAGT
TNF-forward	CAATGGCGTGGAGCTGAGAG
TNF-reverse	GTCTGGTAGGAGACGGCGAT
PTGS1-forward	CGCCAGTGAATCCCTGTTGTT
PTGS1-reverse	AAGGTGGCATTGACAAACTCC
PTGS2-forward	CTGGCGCTCAGCCATACAG
PTGS2-reverse	CGCACTTATACTGGTCAAATCCC
PGES1-forward	TCCTAACCCTTTTGTCGCCTG
PGES1-reverse	CGCTTCCCAGAGGATCTGC
PGES2-forward	GTGACCGAGTTCGGCAATAAG
PGES2-reverse	CGGACAATGTAGTCAAAGGACG
PPARG-forward	GGGATCAGCTCCGTGGATCT
PPARG-reverse	TGCACTTTGGTACTCTTGAAGTT

(Continued on next page)

(Continued)

Table 2-1 Primer list used in Chapter 2

Primer	Sequence
PLIN3-forward	TATGCCTCCACCAAGGAGAG
PLIN3-reverse	ATTCGCTGGCTGATGCAATCT
FCGR1A-forward	ACAGAGGCTGGCTACTACTG
FCGR1A-reverse	GACAGATATTCCTGCTGATGTG
FCGR2B-forward	CCACTAATCCTGATGAGGCTGACA
FCGR2B-reverse	CTCAAATCCCAATGCAAGACAATG
DEFA1, 3-forward	ATGAGGACCCTCGCCATCCTTGCT
DEFA1, 3-reverse	TCAGCAGCAGAATGCCCAGCGTCTTCCC
DEFA4-forward	GTCTGCTCTTGCAGATTAGTATTCTG
DEFA4-reverse	TTAATCGACACGCGTGCAGCAGTAT
HPRT-forward	CCTGGCGTCGTGATTAGTGAT
HPRT-reverse	AGACGTTCAGTCCTGTCCATAA

3.3.3. Phagocytosis assay

Differentiated HL-60 cells were counted and normalized into 1×10^6 live HL-60 cells / 1 mL media in 24 well plate. 10 μL of Latex Beads-Rabbit IgG-PE Complex (Cayman Chemical, MI, USA) were added into each well. The cells with fluorescent beads were incubated for 4 hours at 37 degree in a 5% CO_2 incubator, and then they were wash out free beads from HL-60. Fluorescent analysis was performed by flow cytometer. Data were analyzed by FlowJo software.

3.3.4. T cell proliferation assay

Jurkat cells were stained by CellTrace CFSE Cell Proliferation Kit (ThermoFisher SCIENTIFIC, CA, USA) according to manufacturer's protocol. As a difference to the protocol, the stained cell number was two-fold. Stained Jurkat cells were co-cultured with differentiated HL-60. Their cell number on one well is Jurkat: 5×10^5 cells/well HL-60: 1.25×10^5 or 6.25×10^4 cells/well. Co-cultured media contained 50% conditional media, and 30 unit/mL recombinant IL-2 (PEPROTECH, NJ, USA) and Dynabeads Human T-activator CD3/CD28 were added. The cells were harvested 1, 3, 5 days after co-culture. Fluorescent analysis was performed by flow cytometer. Data were analyzed by FlowJo software.

3.3.5. Antibody-independent Cellular cytotoxicity assay

A549 cells were seeding at 3×10^4 cells/well on 96 well plate. 24 hours after seeding, differentiated HL-60 cells were add 6×10^5 cells/well (Killer:Target = 20:1). Each wells were washed twice by PBS 12 hours after co-culture, and the trypsinized. Live A549 cell number were decided manually by using trypan blue staining.

3.3.6. RNA-seq Library Construction

To construct libraries, the cells were induced to differentiate, and then 1-day and 6-days inducted cells were harvested by TRIzol reagent (ThermoFisher SCIENTIFIC). Library was constructed by 1μg of total RNA to follow Truseq Stranded mRNA Sample preparation Guide by Illumina (San Diego, CA, USA). As a difference, reaction scale was reduced to half. Two paired-end sequencing and a single sequencing run were performed on the illumine Hiseq1500 or Hiseq2500.

3.3.7. Differential expression analysis

Quality check for read data was performed by fastqc v0.11.5. The program HISAT2 (v2.1.0 [72]) was used to align sequencing reads to the reference genome GRCh37. Annotated reference gene abundances were counted using StringTie (v1.3.3b; [73]). Statistical analysis of differential gene expression was conducted with edgeR [74]. Normalization of expression values was performed by TMM method. And fold change was calculated by using generalized linear model for the correction of replicate bias. Differentially expression genes (DEGs) were filtered by False Discovery Rate (FDR) < 0.05 and $\log_2$(Fold-change) > 1.

DEGs were analyzed by Venn diagram calculated by “Calculate and draw custom Venn diagram” (http://bioinformatics.psb.ugent.be/webtools/Venn/). And also, Gene Ontology annotation of DEGs and gene-set Enrichment for pathway analysis were performed by Enrichr (https://amp.pharm.mssm.edu/Enrichr/).

3.4. Results

3.4.1. PPM1D inhibition enhances neutrophil inflammatory response but suppresses the phagocytotic activity

Neutrophils express and secrete the inflammatory cytokines following LPS stimulation, including IL-1β, IL-6, IL-8, TNF-α. The cytokine expression in PPM1D-inhibited HL-60 was analyzed. Differentiated cells —HL-60 cells differentiated by ATRA— expressed *IL1B*, *IL6*, *IL8*, ad *TNF* (**Figure 3-1**). However, PPM1D-inhibited cells —HL-60 differentiated by ATRA and SL-176— expressed higher levels of cytokines compared with differentiated HL-60. This indicated that PPM1D inhibition enhanced the expression of cytokines.

Activated neutrophils rapidly induce apoptosis. Numbers of apoptotic cells after LPS stimulation were analyzed. Increased numbers of apoptotic cells in differentiated cells were increased by LPS stimulation (**Figure 3-2**). Interestingly, PPM1D-inhibited cells showed a small ratio of apoptotic cells before LPS stimulation, which was not increased by LPS stimulation. These results are similar to delayed neutrophil apoptosis, which is seen in tumors or severe chronic inflammation such as sepsis［75］.

Next, IgG-dependent phagocytotic activity, the primary function of neutrophils was analyzed (**Figure 3-3**). Fluorescent beads conjugated with IgG were added into the cell culture, and the amounts of fluorescent beads engulfed by the HL-60 was measured by fluorescent microscopy (**Figure 3-3**). Interestingly, fluorescence in PPM1D-inhibited cells was decreased and flow cytometry analysis showed a decrease in phagocytosis. As discussed in chapter 2, PPM1D inhibition increased the efficiency of myeloid differentiation but repressed. phagocytotic activity and delayed apoptosis. This suggests that PPM1D has biphasic functions on myeloid differentiation and maturation.

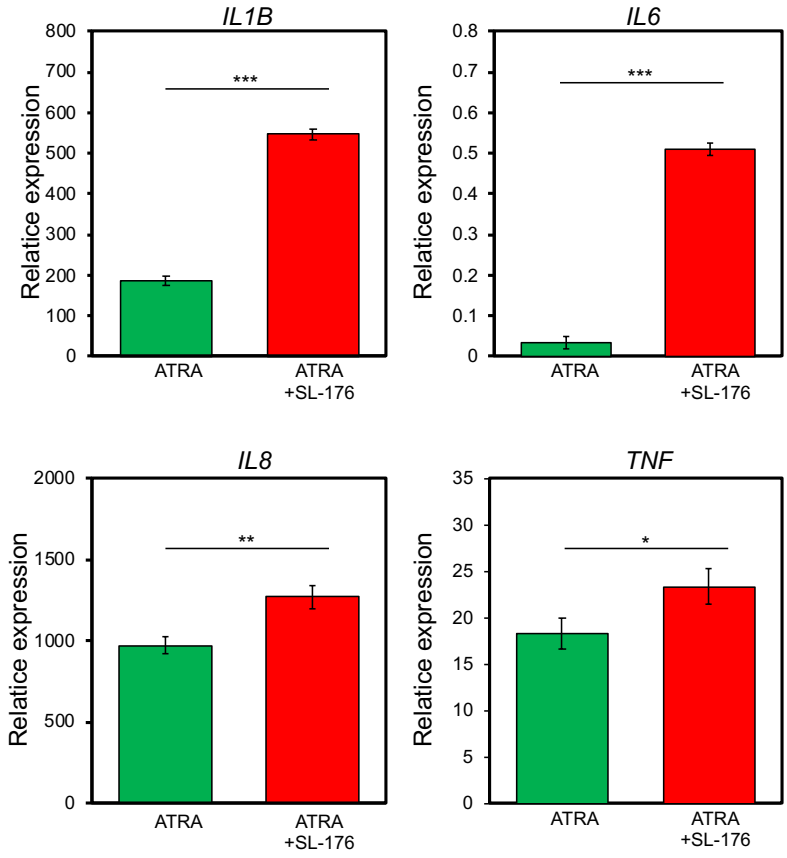

Figure 3-1　Inflammatory cytokine expression

HL-60 cells were treated with 1 μM ATRA with or without for 6 days, and then 1 μg/mL LPS was added. The cells were harvested 12 hours after stimulation. The mRNA levels, IL1B, IL6, IL8, TNF and HPRT were quantitatively analyzed by RT-PCR, and normalized to HPRT mRNA expression. *p<0.05, **p<0.01, ***p<0.001, *t*-test

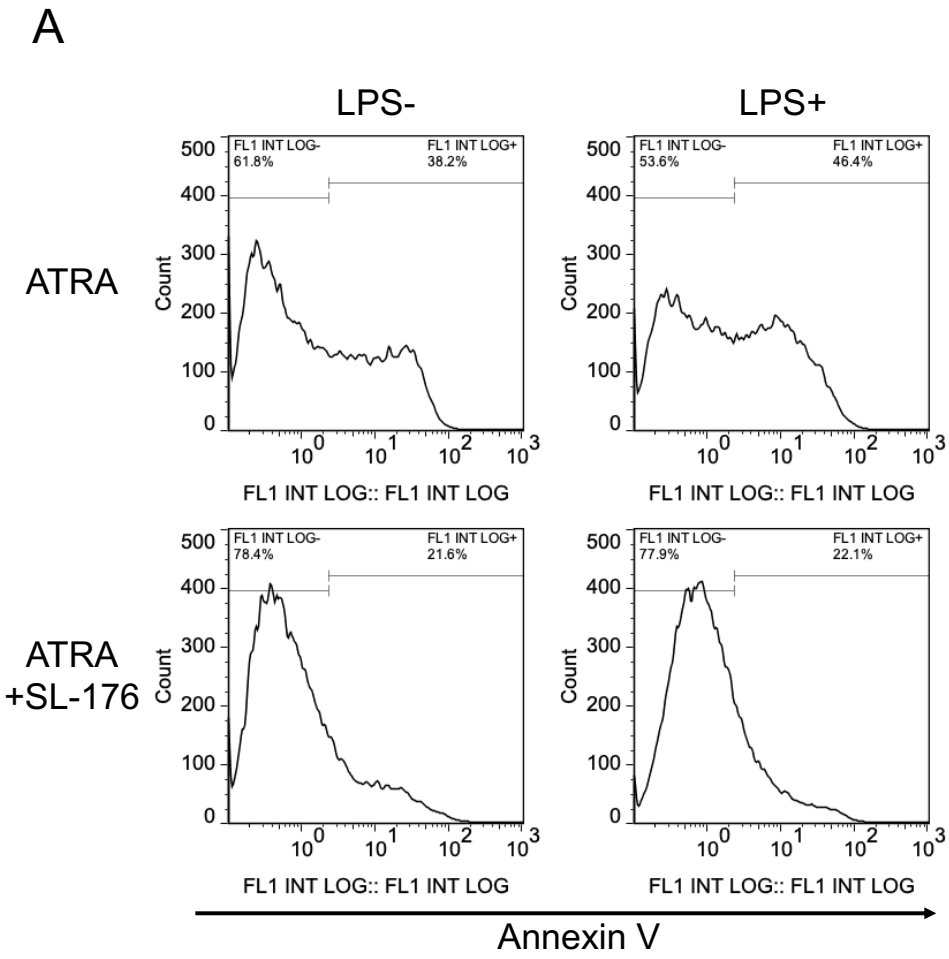

Figure 3-2 PPM1D inhibited HL-60 shows delayed neutrophil apoptosis

HL-60 cells were treated with 1 μM ATRA with or without for 6 days, and then 1 μg/mL LPS was added. The cells were harvested 12 hours after stimulation. The cells were harvested and stained by Annexin V conjugated with FITC. They were analyzed by Flow cytometer. (A) is shown representative data.

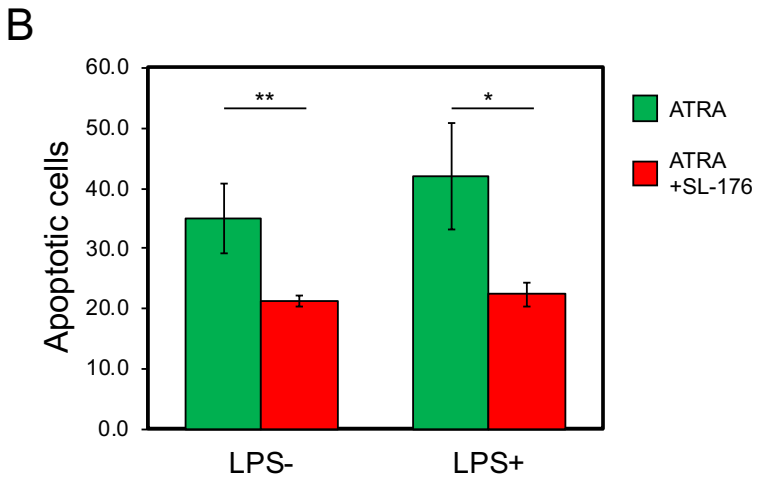

(Continued)

Figure 3-2 PPM1D inhibited HL-60 shows delayed neutrophil apoptosis

(B) is shown the average value on N=3. *p<0.05, **p<0.01, *t*-test

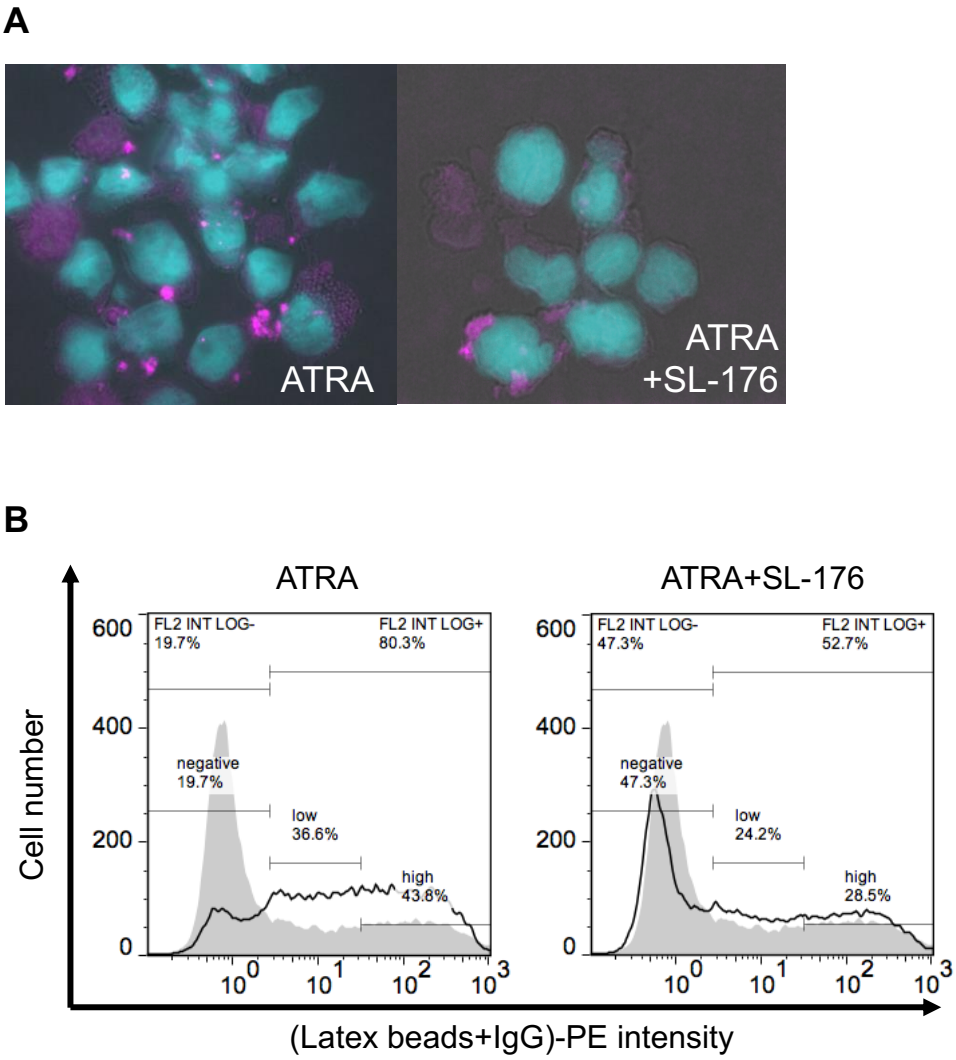

Figure 3-3 Phagocytic capacity of differentiated HL-60 cells with SL-176

HL-60 cells were treated with 1 μM ATRA with or without for 6 days, and then normalized cell number, and IgG-latex beads conjugated PE were added. The cells were harvested 4 hours after. (A) fluorescent image (Cyan: DAPI, Magenta: PE, and bright field images were merged), (B) Fluorescent intensities on single cell were analyzed by flow cytometer. On the histogram, undifferentiated HL-60 was indicated by gray.

3.4.2. PPM1D-inhibited neutrophils suppress T cell growth and cellular cytotoxicity

PPM1D-inhibited cells had increased inflammatory cytokine production, delayed neutrophils apoptosis, and the decreased phagocytotic activity. From these results, it was hypothesized that PPM1D inhibition polarized HL-60 to PMN-MDSC.

Next, I checked the function of PPM1D-inhibited cells on T-cell proliferation, which is the primary function of PMN-MDSC, was analyzed. Antigen is presented to T cells by APC, T cells produce autocrine IL-2, which promotes T cell clonal selection and proliferation. However, MDSC inhibits T cell proliferation and represses immune responses ［71］. The Jurkat cell line, a lymphoblast derived from acute T cell leukemia, was used as a model for T cells. Jurkat cells and HL-60 cells were co-cultured in the presence of IL-2, and anti-CD3 and anti-CD28 monoclonal antibodies (**Figure 3-4**). Differentiated cells did not affect Jurkat cell growth. However, Jurkat cells co-cultured with PPM1D-inhibited cells showed repressed proliferation. Thus, PPM1D-inhibited cells acquired T cell proliferation suppressive activity.

Fridlender Z. G. *et al*. (2009) reported that neutrophils killed the non-small cell lung cancer cells ［76］. Therefore, human lung cancer A549 cells were used for experiments to investigate whether neutrophils affect other types of cancer cells. Differentiated cells or PPM1D-inhibited cells were added into A549 culture dishes 24 hours after seeding. The members of A549 cells in each well were counted after 12 hours (**Figure 3-5**). Differentiated cells killed approximately 45% of A549 cells, but PPM1D-inhibited cells were only decreased by approximately 10%. Therefore, PPM1D-inhibited cells acquired a phenotype similar to PMN-MDSC.

3.4.3. PPM1D inhibition strongly promotes the production of prostaglandin E_2

Veglia F. *et al*. found that PMN-MDSC contained more PGE_2 compared with neutrophils. Moreover, they reported that the treatment of neutrophils with arachidonic

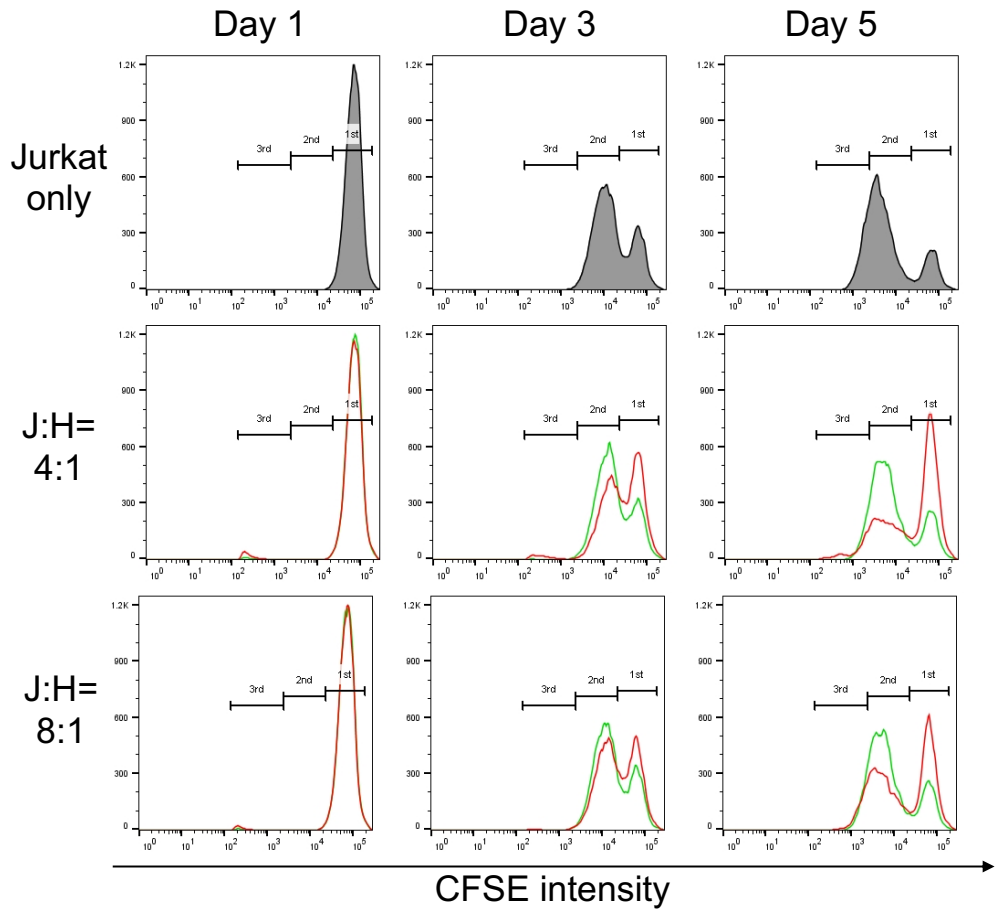

Figure 3-4 T cell proliferation assay

HL-60 cells were treated with 1 μM ATRA with or without SL-176 for 6 days, and then the cells were washed cells and co-cultured with Jurkat cells on the indicated ratio. Jurkat cells were labeled by CFSE. Each day, the cells were harvested and analyzed by flow cytometer. Green line shows Jurkat cells incubated with Differentiated cells. Red line shows Jurkat cells incubated with PPM1D-inhibited cells.

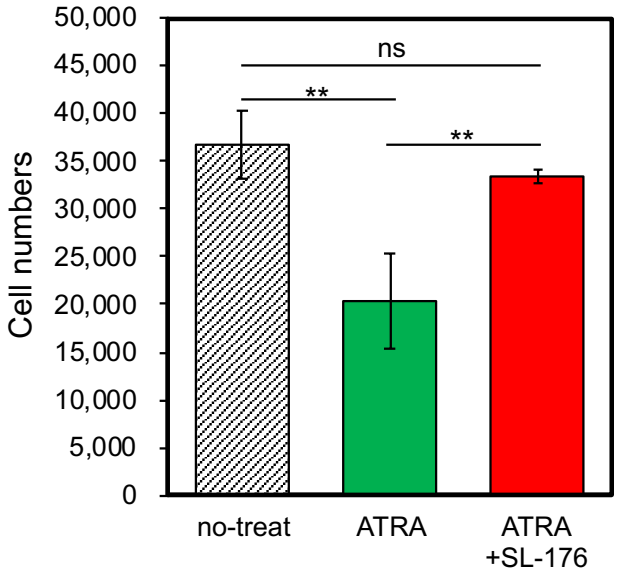

Figure 3-5　Analysis of HL-60's Cellular Cytotoxicity against human lung cancer cell line A549

HL-60 cells were treated with 1 μM ATRA with or without SL-176 for 6 days, and then the cells were washed and co-cultured with A549 cells in the ration of 1:20. The cells were trypsinized and counted 12 hours after. No-treat condition is to culture A549 only. The y-axis indicated the average value of three experiments, ns: not significant, **$p<0.01$, *t*-test.

acid, a PGE_2 precursor, enhanced their immunosuppressive activity. Next, the regulation of LPS-induced PGE_2 was assessed. Differentiated cells or PPM1D-inhibited cells were incubated for 12 hours in fresh media with 1 mg/mL LPS. Supernatant from each group was harvested and quantified by ELISA (**Figure 3-6**). PPM1D-inhibited cells produced 15 times more PGE_2 than differentiated cells. qPCR analysis revealed that COX-2 and mPGES-1 expression levels were increased (**Figure 3-7**). Of note, COX-2 and mPGES-1 were reported to be upregulated in several tumors and therefore might be promising drug targets for chronic inflammation similar to those for Celecoxib ［77］.

Next, the amount of lipid in HL-60 cells was assessed by oil red O staining. Prostaglandin is synthesized from arachidonic acid (AA), a carboxylic acid with a 20-carbon long chain and four *cis*-double bonds. AA is prepared from linoleic acid (18:2($\Delta^{9,12}$)) and DAG. Oil red O staining showed that PPM1D-inhibited cells contained more lipid than differentiated cells (**Figure 3-7**). Furthermore, PPAR-γ and perilipin-3, a transcriptional factor and lipid droplet-associated protein, respectively, were increased in PPM1D-inhibited cells (**Figure 3-8**). This suggested that lipid droplet formation in HL-60 was enhanced by PPM1D inhibition.

Taken together, these results indicate that PPM1D regulates PMN-MDSC polarization via eicosanoid metabolism. PPM1D inhibition induced PGE_2 production by increasing of COX-2/mPGES-1 and enhancing of lipid droplet formation, which may polarize neutrophils into PMN-MDSC by an autocrine pathway

3.4.4. The transcriptional basis of PMN-MDSC-like cell formation by PPM1D repression

Next, transcriptome analysis for PMN-MDSC-like HL-60 cells were performed. Total RNA was extracted from HL-60 cells treated with differentiation stimuli for 1 or 6 days, and poly A tailed mRNA were purified and analyzed by RNA-seq (Illumine).

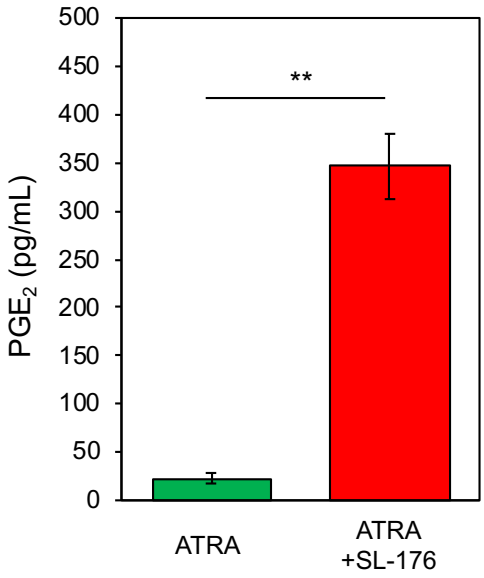

Figure 3-6 Quantification of Prostaglandin E_2 by ELISA

HL-60 cells were treated with 1 μM ATRA with or without SL-176 for 6 days, and then the cells were washed and cultured in flesh media without serum. The supernatants were collected 12 hours after. **p<0.01, *t*-test

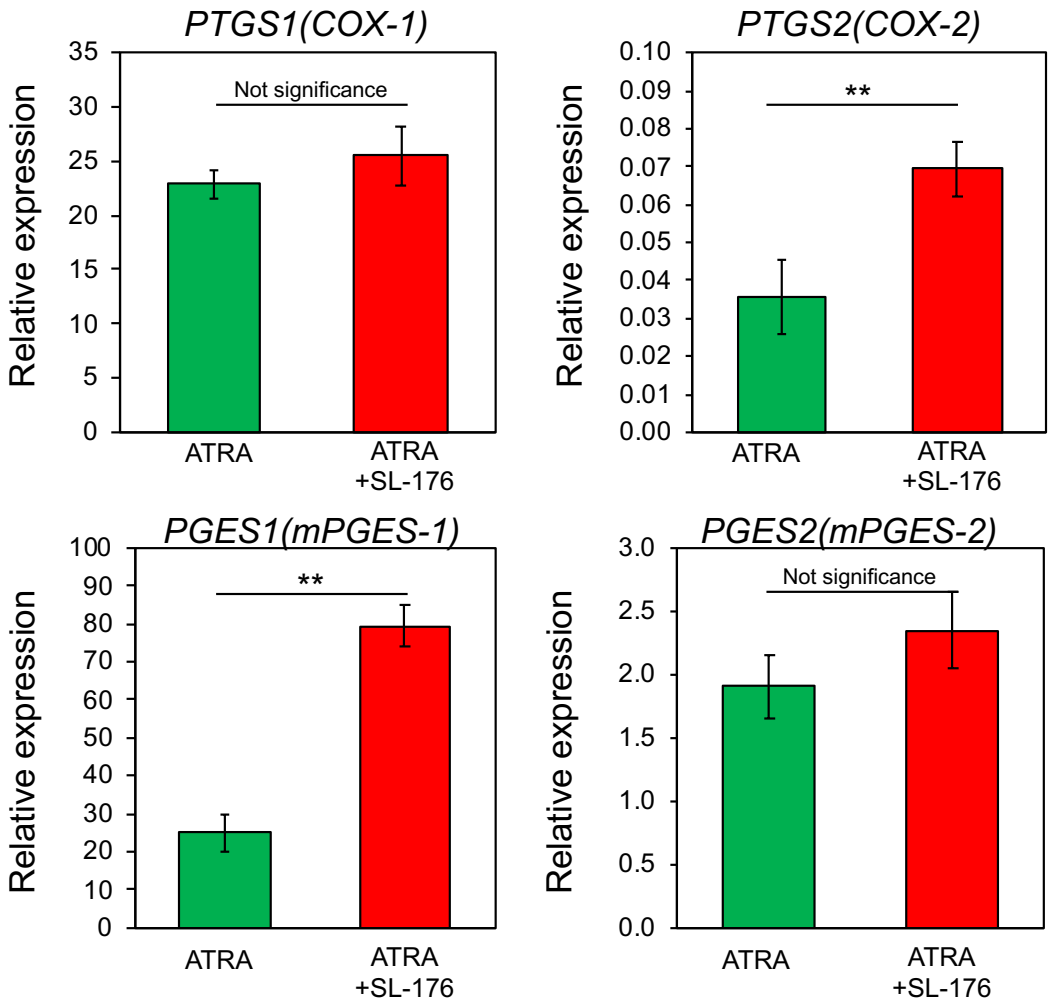

Figure 3-7 mRNA transcription on Prostaglandin synthesis in HL-60

HL-60 cells were treated with 1 μM ATRA with or without SL-176 for 6 days, and then the cells were harvested. The mRNA levels of PTGS1, PTGS2, PGES1, PGES2 and HPRT were quantitatively analyzed by RT-PCR and normalized to HPRT mRNA expression. **p<0.01, *t*-test All data were shown the average of three independent experiments.

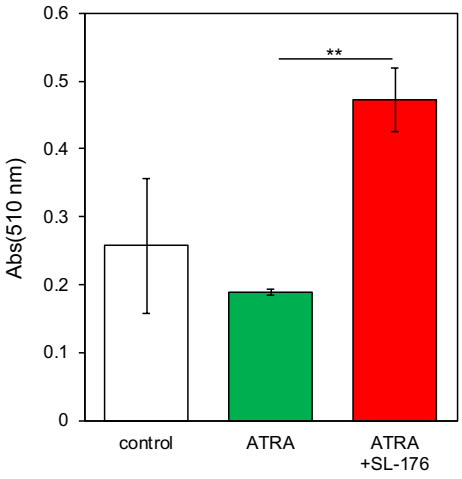

Figure 3-8　Measurement of cellular lipid amount by Oil red O staining for HL-60

HL-60 cells were treated with 1 μM ATRA with or without SL-176 for 6 days, and then oil red O staining was performed. The extract from stained HL-60 was measured on 510 nm. Data represent the mean±SD of three independent experiments. **p<0.01, *t*-test

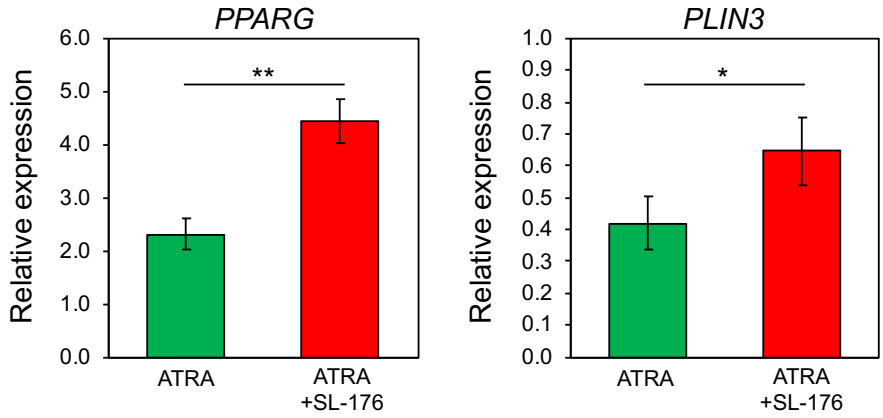

Figure 3-9 mRNA transcription on lipid metabolism in PPM1D-inhibited HL-60

HL-60 cells were treated with 1 μM ATRA with or without SL-176 for 6 days, and then the cells were harvested. The mRNA levels of PPARG, PLIN3, and HPRT were quantitatively analyzed by RT-PCR and normalized to HPRT mRNA expression. **p<0.01, *t*-test All data were shown the average of three independent experiments.

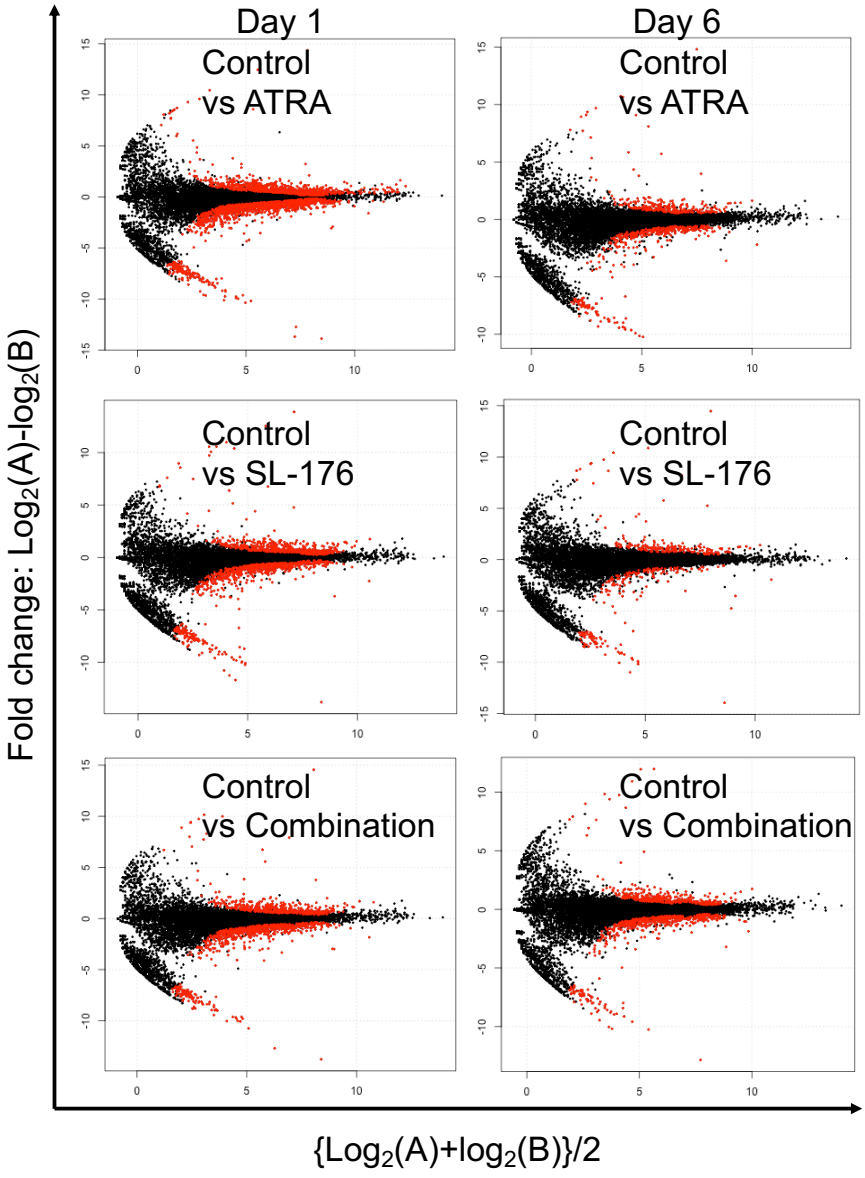

Figure 3-10　MA plots for each sample against control HL-60

Inset labels “A vs B” indicates two comparing groups, x-axis indicates the average of two logarithm to the base 2 of two comparing group, and y-axis indicates a logarithm to the base 2 of fold change. The plots show one gene. Every groups are the average of three independent experiments. Genes indicated red point are False discovery rate < 0.05.

Figure 3-10 shows MA plots for each sample. Red dots indicate genes in which the FDR is under 0.05. Differential expression analysis was performed and compared between each condition (**Figure 3-11)**. Differential expression genes (DEGs) were analyzed in PMN-MDSC-like HL-60 and compared with differentiated cells every day and followed by GO analysis or pathway analysis (**Table 3-2, 3, 4, 5, 6, 7**). Gene sets related to phagocytosis, inflammation, and lipid metabolism such as PPAR signals were enriched in PMN-MDSC-like cells. PMN-MDSC-like cells may change their phenotypes at the transcriptional level.

Moreover, gene sets related to IgG-dependent phagocytosis and cellular cytotoxicity were different between differentiated cells and PMN-MDSC-like cells on day 6 (**Figure 3-12, Figure 3-13**). IgG-dependent phagocytosis is mediated by FCGR. FCGR1A has an ITAM motif and promotes phagocytosis whereas FCGR2B has an ITIM motif and inhibits phagocytosis. Quantitative RT-PCR revealed gene expressions were changed when phagocytosis was repressed (**Figure 3-14**). Regarding cellular cytotoxicity, anti-biotic peptide alpha-defensin disturbs the cellular membrane and kills bacteria or damaged tissues. PMN-MDSC cells had decreased its DEFA1, 3 and DEFA4 expression levels (**Figure 3-15**). Taken together, PPM1D inhibition induced changes in neutrophils at the transcriptional level, suggesting PPM1D maintain the functions of neutrophil subtypes.

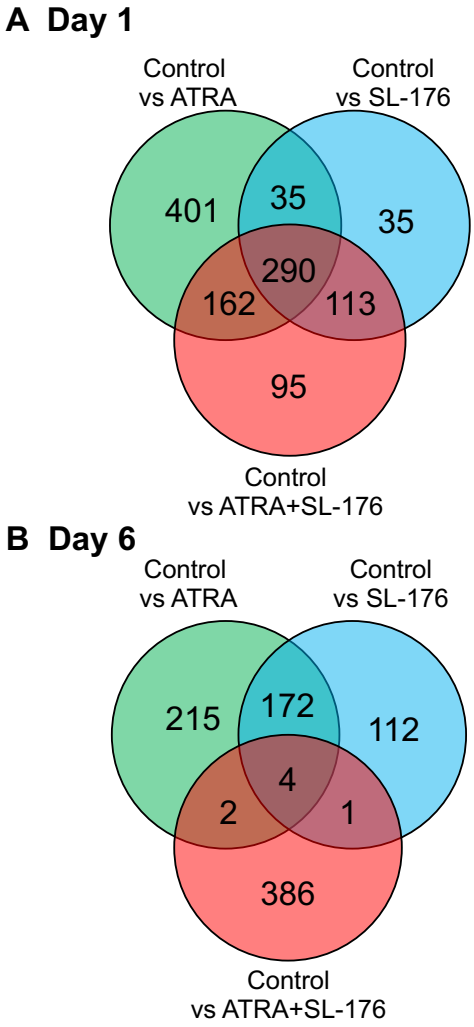

Figure 3-11 Venn diagram for DEGs in HL-60

Differential expression genes (DEGs) were calculated by False discovery rate (FDR)<0.05 and the logarithm to the base 2 of fold change (log_2FC) >1.

Table 3-2 Gene ontology analysis in comparison between ATRA and ATRA+SL-176 at Day 1

rank	Term	P-value
1	regulation of cellular macromolecule biosynthetic process (GO:2000112)	1.29E-06
2	regulation of nucleic acid-templated transcription (GO:1903506)	9.23E-06
3	regulation of gene expression (GO:0010468)	2.36E-05
4	peptidyl-serine phosphorylation (GO:0018105)	5.68E-05
5	ERBB signaling pathway (GO:0038127)	1.70E-04
6	protein phosphorylation (GO:0006468)	3.25E-04
7	amino sugar metabolic process (GO:0006040)	5.79E-04
8	N-acetylneuraminate metabolic process (GO:0006054)	5.79E-04
9	phosphorylation (GO:0016310)	6.98E-04
10	epidermal growth factor receptor signaling pathway (GO:0007173)	7.72E-04
11	peptidyl-serine modification (GO:0018209)	1.15E-03
12	regulation of actomyosin structure organization (GO:0110020)	1.27E-03
13	ERBB2 signaling pathway (GO:0038128)	1.43E-03
14	JNK cascade (GO:0007254)	2.20E-03
15	microvillus organization (GO:0032528)	0.00377
16	microvillus assembly (GO:0030033)	0.00377
17	deadenylation-dependent decapping of nuclear-transcribed mRNA (GO:0000290)	0.00377
18	protein autophosphorylation (GO:0046777)	0.00391

(Continued on next page)

(Continued)

Table 3-2 Gene ontology analysis in comparison between ATRA and ATRA+SL-176 at Day 1

rank	Term	P-value
19	internal peptidyl-lysine acetylation (GO:0018393)	0.00533
20	type B pancreatic cell differentiation (GO:0003309)	0.00547
21	inositol metabolic process (GO:0006020)	0.00547
22	anion transmembrane transport (GO:0098656)	0.00641
23	plasma membrane bounded cell projection morphogenesis (GO:0120039)	0.00729
24	tryptophan metabolic process (GO:0006568)	0.00757
25	regulation of neuroblast proliferation (GO:1902692)	0.00757
26	MyD88-dependent toll-like receptor signaling pathway (GO:0002755)	0.00846
27	plasma membrane bounded cell projection assembly (GO:0120031)	0.00863
28	cellular response to DNA damage stimulus (GO:0006974)	0.00874
29	regulation of cell development (GO:0060284)	0.00948
30	regulation of transcription, DNA-templated (GO:0006355)	0.00967

Gene ontology analysis was performed for the DEGs in the comparison of transcriptome between differentiated cells and PPM1D-inhibited cells, 1-day treatment. For the analysis, I performed GO annotation on Enrichr web site. [78], arrangement in the order of p-value, and Top 30 were shown.

Table 3-3 Gene ontology analysis in comparison between ATRA and ATRA+SL-176 at Day 6

rank	Term	P-value
1	phospholipid translocation (GO:0045332)	5.55E-05
2	lipid translocation (GO:0034204)	7.06E-05
3	phospholipid transport (GO:0015914)	2.00E-04
4	cytoskeletal anchoring at nuclear membrane (GO:0090286)	4.47E-04
5	interleukin-1 beta secretion (GO:0050702)	4.47E-04
6	regulation of cell development (GO:0060284)	6.56E-04
7	nuclear migration (GO:0007097)	6.60E-04
8	interleukin-1 beta production (GO:0032611)	6.60E-04
9	interleukin-1 secretion (GO:0050701)	6.60E-04
10	plasma membrane bounded cell projection morphogenesis (GO:0120039)	7.37E-04
11	positive regulation of ERBB signaling pathway (GO:1901186)	0.00114
12	ERBB2 signaling pathway (GO:0038128)	0.00130
13	entry of bacterium into host cell (GO:0035635)	0.00165
14	positive regulation of cholesterol efflux (GO:0010875)	0.00211
15	cellular response to low-density lipoprotein particle stimulus (GO:0071404)	0.00211
16	negative regulation of type I interferon production (GO:0032480)	0.00222
17	protein targeting to vacuole (GO:0006623)	0.00243

(Continued on next page)

(Continued)

Table 3-3 Gene ontology analysis in comparison between ATRA and ATRA+SL-176 at Day 6

rank	Term	P-value
18	positive regulation of Wnt signaling pathway (GO:0030177)	0.002583
19	lytic vacuole organization (GO:0080171)	0.00277
20	vacuolar transport (GO:0007034)	0.00315
21	positive regulation of epidermal growth factor receptor signaling pathway (GO:0045742)	0.00315
22	MyD88-dependent toll-like receptor signaling pathway (GO:0002755)	0.00315
23	stress-activated protein kinase signaling cascade (GO:0031098)	0.00337
24	regulation of interferon-alpha production (GO:0032647)	0.00395
25	lysosome organization (GO:0007040)	0.00400
26	positive regulation of cholesterol transport (GO:0032376)	0.00472
27	negative regulation of cell development (GO:0010721)	0.00472
28	regulation of lipid metabolic process (GO:0019216)	0.00483
29	protein acetylation (GO:0006473)	0.00500
30	entry into host cell (GO:0030260)	0.00500

Gene ontology analysis was performed for the DEGs in the comparison of transcriptome between differentiated cells and PPM1D-inhibited cells, 6-days treatment. For the analysis, I performed GO annotation on Enrichr web site., arrangement in the order of p-value, and Top 30 were shown.

Table 3-4 Pathway analysis in comparison between ATRA and ATRA +SL-176 at Day 1 by using NCATS BioPlanet

rank	Term	P-value
1	Generic transcription pathway	1.76E-08
2	RORA activates circadian expression	1.12E-06
3	BMAL1-CLOCK/NPAS2 activates circadian expression	3.24E-06
4	Signaling by constitutively active EGFR	8.49E-06
5	Circadian rhythm	1.10E-05
6	PPAR-gamma coactivator role in obesity and thermogenesis	1.58E-05
7	YAP1- and WWTR1 (TAZ)-stimulated gene expression	8.51E-05
8	Non-small cell lung cancer	8.78E-05
9	Control of gene expression by vitamin D receptor	1.11E-04
10	Lipid metabolism regulation by peroxisome proliferator-activated receptor alpha (PPAR-alpha)	3.19E-04
11	EGFR transactivation by gastrin	3.60E-04
12	Transcriptional regulation of white adipocyte differentiation	4.35E-04
13	Mechanism of gene regulation by peroxisome proliferators via PPAR-alpha	6.78E-04
14	Estrogen receptor transcription factor targets	6.83E-04
15	Retinoic acid receptor-mediated signaling	0.00152
16	ERBB1 internalization pathway	0.00165
17	Gene expression	0.00181

(Continued on next page)

(Continued)

Table 3-4 Pathway analysis in comparison between ATRA and ATRA +SL-176 at Day 1 by using NCATS BioPlanet

rank	Term	P-value
18	ERBB1 downstream pathway	0.00199
19	Fanconi anemia pathway	0.00207
20	T cell receptor/Ras pathway	0.00240
21	TRAF3-dependent IRF activation pathway	0.00240
22	T cell signal transduction	0.00291
23	Signaling by EGFR in cancer	0.00294
24	Renal cell carcinoma	0.00298
25	TRAF6-mediated induction of TAK1 complex	0.00316
26	TrkA receptor signaling pathway	0.00316
27	PDGFB signaling pathway	0.00372
28	Cellular response to hypoxia	0.00376
29	Downregulation of ERBB4 signaling	0.00377
30	Transport of nucleotide sugars	0.00377

Pathway analysis was performed for the DEGs which were described in the NOTE of Table 3-1, arrangement in the order of p-value, and Top 30 were shown.

Table 3-5 Pathway analysis in comparison between ATRA and ATRA +SL-176 at Day 6 by using NCATS BioPlanet

rank	Term	P-value
1	Signaling by constitutively active EGFR	3.28E-05
2	Circadian rhythm	2.73E-04
3	Lipid metabolism regulation by peroxisome proliferator-activated receptor alpha (PPAR-alpha)	5.10E-04
4	Transcriptional regulation of white adipocyte differentiation	0.00102
5	BMAL1-CLOCK/NPAS2 activates circadian expression	0.00102
6	Signaling by ERBB2	0.00121
7	Signaling by EGFR in cancer	0.00208
8	RORA activates circadian expression	0.00212
9	Initiation of the second proteolytic cleavage of Notch receptor by receptor-ligand binding	0.00264
10	Statin pathway	0.00277
11	Activation of IRF3/IRF7 mediated by TBK1/IKK epsilon	0.00326
12	Association of licensing factors with the pre-replicative complex	0.00326
13	TRAF6-mediated induction of TAK1 complex	0.00326
14	HDL-mediated lipid transport	0.00326
15	Sprouty regulation of FGF signaling	0.00395
16	KIT signaling regulation	0.00395
17	Negative regulators of RIG-I/MDA5 signaling	0.00448

(Continued on next page)

(Continued)

Table 3-5 Pathway analysis in comparison between ATRA and ATRA +SL-176 at Day 6 by using NCATS BioPlanet

rank	Term	P-value
18	Signaling by FGFR in disease	0.00499
19	Fatty acid, triacylglycerol, and ketone body metabolism	0.00969
20	Downregulation of ERBB4 signaling	0.0108
21	HIF-1 transcriptional activity in hypoxia	0.0114
22	Generic transcription pathway	0.0117
23	Signaling by the B cell receptor (BCR)	0.0129
24	EGFR transactivation by gastrin	0.0137
25	Mitochondrial pathway of apoptosis: multidomain Bcl-2 family	0.0153
26	YAP1- and WWTR1 (TAZ)-stimulated gene expression	0.0157
27	Fanconi anemia pathway regulation	0.0169
28	IKK complex recruitment by IRAK1	0.0169
29	IRAK2-mediated activation of TAK1 complex	0.0169
30	EGFR downregulation	0.0174

Pathway analysis was performed for the DEGs which were described in the NOTE of Table 3-2. Arrange in the order of p-value, and Top 30 were shown.

Table 3-6 Pathway analysis in comparison between ATRA and ATRA +SL-176 at Day 1 by using KEGG pathway

rank	Term	P-value
1	Herpes simplex virus 1 infection	1.99E-05
2	Thyroid hormone signaling pathway	3.68E-05
3	Non-small cell lung cancer	4.87E-04
4	Choline metabolism in cancer	0.00110
5	Renal cell carcinoma	0.00270
6	Human cytomegalovirus infection	0.00866
7	Apoptosis	0.00879
8	Phosphatidylinositol signaling system	0.0101
9	ErbB signaling pathway	0.0107
10	Hepatitis B	0.0108
11	FoxO signaling pathway	0.0115
12	Axon guidance	0.0116
13	mTOR signaling pathway	0.0141
14	Glioma	0.0150
15	Pancreatic cancer	0.0150
16	Chronic myeloid leukemia	0.0162
17	N-Glycan biosynthesis	0.0197
18	Prostate cancer	0.0237
19	Long-term potentiation	0.0246
20	Breast cancer	0.0249
21	Fc epsilon RI signaling pathway	0.0264
22	B cell receptor signaling pathway	0.0325
23	Endometrial cancer	0.0377

(Continued on next page)

(Continued)

Table 3-6 Pathway analysis in comparison between ATRA and ATRA +SL-176 at Day 1 by using KEGG pathway

rank	Term	P-value
24	VEGF signaling pathway	0.0405
25	Cellular senescence	0.0436
26	Kaposi sarcoma-associated herpesvirus infection	0.0586
27	Acute myeloid leukemia	0.0638
28	T cell receptor signaling pathway	0.0693
29	Insulin signaling pathway	0.0714
30	Aldosterone-regulated sodium reabsorption	0.0731

Pathway analysis was performed for the DEGs which were described in the NOTE of Table 3-1. Arrange in the order of p-value, and Top 30 were shown.

Table 3-7 Pathway analysis in comparison between ATRA and ATRA +SL-176 at Day 6 by using KEGG pathway

rank	Term	P-value
1	Cholesterol metabolism	0.00354
2	Sulfur metabolism	0.0137
3	Parkinson disease	0.0275
4	Phagosome	0.0378
5	Huntington disease	0.0464
6	Estrogen signaling pathway	0.0637
7	Inositol phosphate metabolism	0.0659
8	PPAR signaling pathway	0.0659
9	Nucleotide excision repair	0.0719
10	Malaria	0.0794
11	N-Glycan biosynthesis	0.0832
12	Thyroid hormone signaling pathway	0.0911
13	Colorectal cancer	0.101
14	Legionellosis	0.103
15	Gap junction	0.107
16	Salivary secretion	0.114
17	Hepatitis B	0.120
18	GnRH signaling pathway	0.124
19	Circadian rhythm	0.132
20	Oxidative phosphorylation	0.139
21	Cytosolic DNA-sensing pathway	0.139
22	Alzheimer disease	0.141
23	Choline metabolism in cancer	0.146

(Continued on next page)

(Continued) Table 3-7 Pathway analysis in comparison between ATRA and ATRA +SL-176 at Day 6 by using KEGG pathway

rank	Term	P-value
24	Phosphatidylinositol signaling system	0.146
25	Cortisol synthesis and secretion	0.149
26	Mitophagy	0.149
27	Regulation of actin cytoskeleton	0.152
28	Sulfur relay system	0.153
29	SNARE interactions in vesicular transport	0.154
30	Acute myeloid leukemia	0.154

Pathway analysis was performed for the DEGs which were described in the NOTE of Table 3-2. Arrange in the order of p-value, and Top 30 were shown.

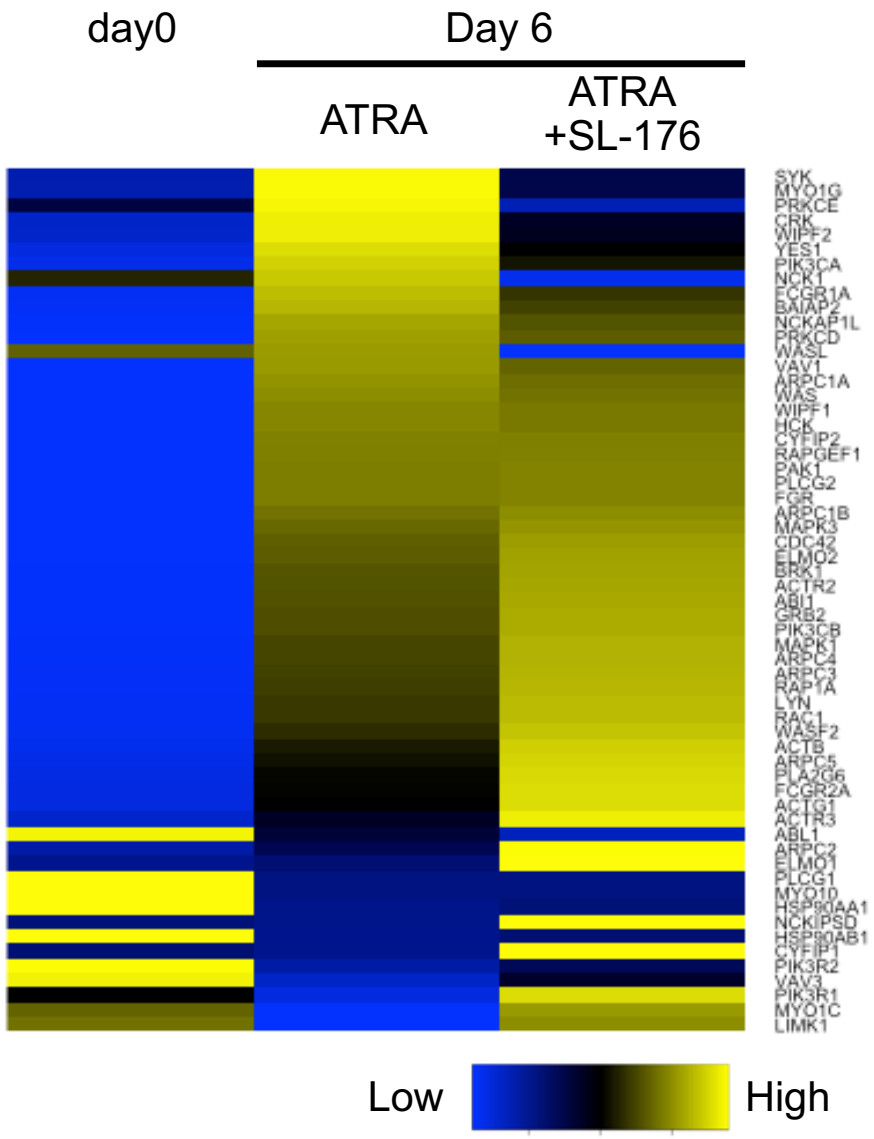

Figure 3-12 Heat map of the expression profile of gene set "FcγR-mediated Phagocytosis"

Each row indicates one gene and gene name is written in right column. Genes was derived from Hsa04666, KEGG pathway. Arrangement in order of expression level on ATRA-treated cells.

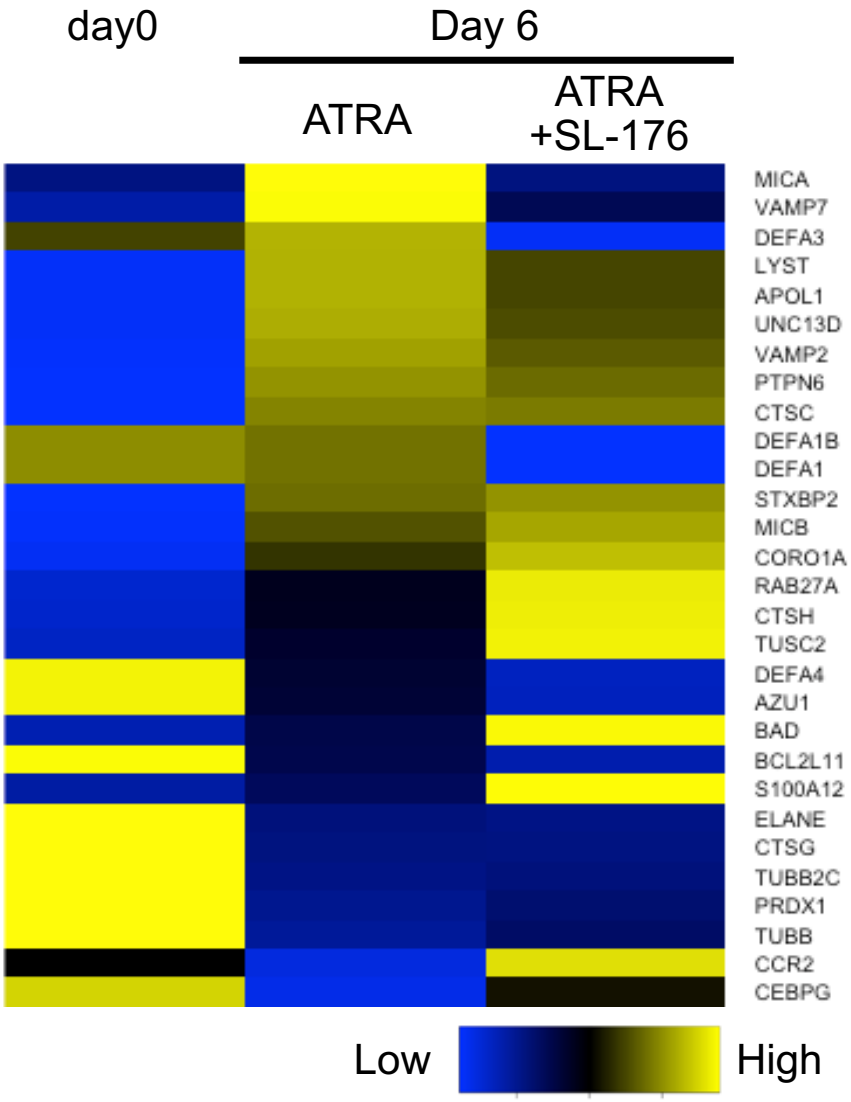

Figure 3-13 Expression profile of Gene set "cell killing"

Each row indicates one gene and gene name is written in right column. Genes was derived from 0001906, Gene ontology consortium. Arrangement in order of expression levels on ATRA-treated cells.

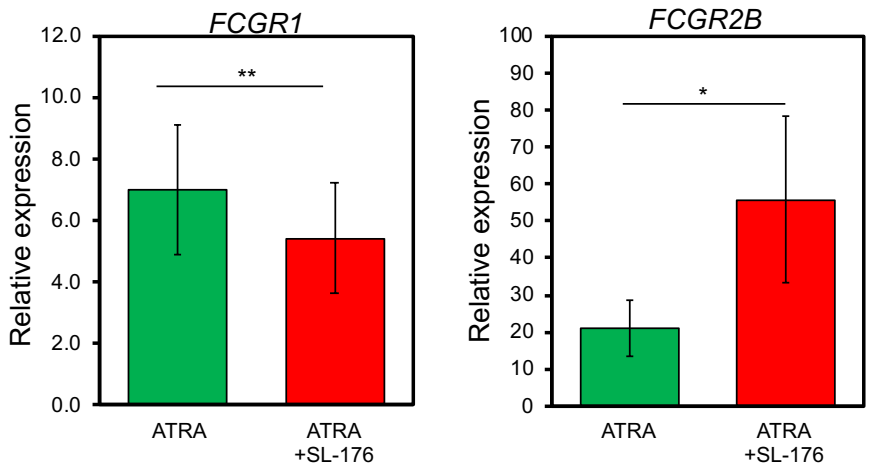

Figure 3-14 Receptor gene expression related with Phagocytic ability of differentiated HL-60 cells with PMN-MDSC like cells

HL-60 cells were treated with 1 μM ATRA with or without SL-176 for 6 days, and then the cells were harvested. The mRNA levels of FCGR1, FCGR2B, and HPRT were quantitatively analyzed by RT-PCR and normalized to HPRT mRNA expression. *p<0.05, **p<0.01, *t*-test. All data were shown the average of three independent experiments.

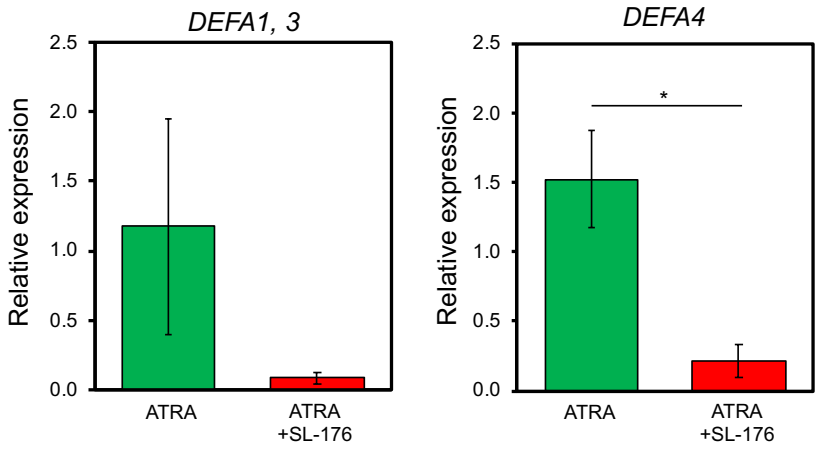

Figure 3-15 Anti-bacterial peptide gene expression related with cellular cytotoxicity of differentiated HL-60 cells with PMN-MDSC like cells

HL-60 cells were treated with 1 μM ATRA with or without SL-176 for 6 days, and then the cells were harvested. The mRNA levels of DEFA1, 3, DEFA4, and HPRT were quantitatively analyzed by RT-PCR and normalized to HPRT mRNA expression. *p<0.05, *t*-test All data were shown the average of three independent experiments.

3.5. Discussion

In chapter 2, it was demonstrated that PPM1D inhibition induced myeloid differentiation and enhanced ATRA-induced differentiation. In this chapter, the PPM1D function in differentiated HL-60 was analyzed. LPS stimulation, a model of sepsis shock, induced inflammatory cytokine expression in HL-60, and PPM1D inhibition enhanced their expressions. However, numbers of apoptotic cells were decreased after LPS stimulation suggesting PPM1D inhibition induced a severe and chronic inflammatory response from neutrophils. Furthermore, cytokines, especially IL-6, are inducers of chronic inflammation in cancer patients ［79］.

Phagocytosis is a critical function of neutrophils. IgG-dependent phagocytosis is also critical for immune therapies. Dr. Appella's group reported that T cell and B cell functions were reduced in *Ppm1d* knockout mice. Taken together, PPM1D may act as a positive regulator of the crosstalk between innate and adaptive immunity.

T cell proliferation is an essential mechanism for adaptive immunity. PMN-MDSCs inhibit proliferation, and tumorigenesis may bypass T cell responses by inducing PMN-MDSC. Veglia *et al*. reported that tumor size growth was strongly repressed by the depletion of PMN-MDSC and rescued by T cell depletion using the anti-CD8 antibodies. In this chapter, PPM1D-inhibited cells repressed T cell proliferation but promoted cancer cell growth. These results indicate PPM1D specifically inhibits T cell growth and induces a PMN-MDSC-like phenotypes.

Veglia *et al*. reported that FATP2, a transporter that uptakes long-chain fatty acids, was overexpressed in PMN-MDSC, and increased the intracellular amount of PGE_2 to generate immunosuppressive neutrophils. Moreover, Cuartero's group reported a PPAR-γ agonist rosiglitazone induced polarization into N2 type neutrophils ［26］. This chapter demonstrated that PGE_2 production was markedly increased in PPM1D-inhibited cells (Figure 3-16). Furthermore, quantitative RT-PCR analysis showed a significant increase

in genes involved in LD formation including PPARG and PLIN3, and the PGE_2 synthetases COX-2 and mPGES-1 significantly. Furthermore, PPM1D inhibition increased cellular lipids. Therefore, PPM1D may regulate polarization to PMN-MDSC via the lipid metabolism of eicosanoids.

In summary, PPM1D inhibition polarized neutrophils into an immunosuppressive subset via the promotion of PGE_2 production. It is important to clarify the PPM1D substrate for the immune therapies against tumors.

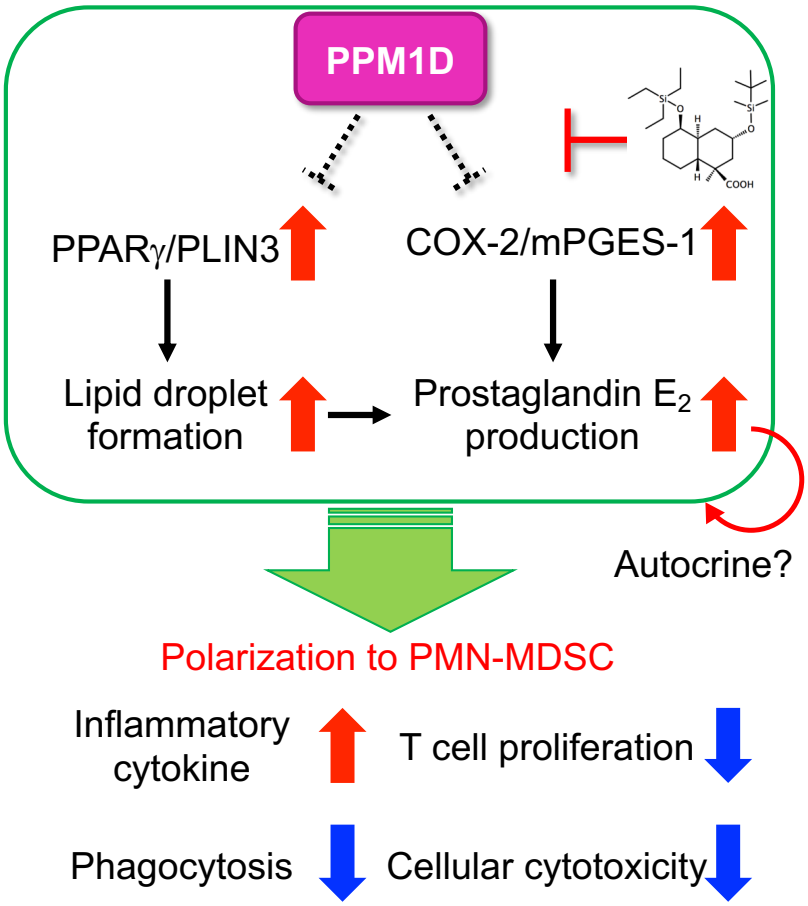

Figure 3-16　PPM1D inhibition promote myeloid differentiation, its maturation and the polarization into PMN-MDSC

PPM1D inhibition changed lipid metabolism in HL-60 cells. Expression levels related to lipid droplet formation and eicosanoid metabolism are increased by PPM1D inhibition. Finally, PGE_2 production was enhanced, and then induced polarization to PMN-MDSC.

4. Conclusion

Neutrophils have critical roles in the early stages of innate immunity by killing bacteria via phagocytosis, producing anti-bacterial molecules such as ROS or defensin, and secreting cytokines or lipid mediators that activate or repress other immune cells. Recently, neutrophils were reported to have functional heterogeneity, with some subsets showing immunosuppressive effects. Protein phosphatase is thought to have an essential role in various cell types in healthy tissues. Leukocytes contain a specific alternative splicing variant of PPM1D. This study demonstrated that PPM1D is involved in myeloid differentiation and polarization into PMN-MDSC. Furthermore, results from this study suggest a model whereby PPM1D maintains a normal neutrophil state via the repression of PGE_2 synthesis and secretion.

In chapter 2, the effect of our small molecule PPM1D inhibitor, SL-176, on an acute myeloid leukemia cell line HL-60 was investigated. We developed a novel fluorescent compound TAP-4PH as a probe to visualize cellular shapes and morphologies. It was demonstrated that PPM1D inhibition induced myeloid differentiation but not monocytic differentiation. SL-176 treated cells had an increased ratio of the G1/G0 phase cells. These results suggest that PPM1D represses myeloid differentiation. This report is consistent with previous reports. Our previous report demonstrated that SL-176 repressed the cellular proliferation of PPM1D overexpressing cells in lung and breast cancer. HL-60 cells express PPM1D at a normal level. Therefore, SL-176 might arrest the cell cycle of HL-60 by inducing myeloid differentiation.

In chapter 3, it was found that PPM1D inhibition promoted inflammation and delayed apoptosis. However, it strongly repressed IgG-dependent phagocytosis, cellular cytotoxicity, and inhibited T cell proliferation. Moreover, PGE_2 production was markedly increased in PPM1D-inhibited cells. Furthermore, genes related to lipid droplet formation and PGE_2 synthesis were increased in PPM1D-inhibited cells. These results suggest that

PPM1D downregulates PPARG and PLIN3 in neutrophils and represses PGE_2 synthesis; moreover, PGE_2 induces to polarization into PMN-MDSC.

Transcriptome analysis revealed PPM1D-inhibited cells differentially expressed inflammatory-related and lipid metabolism-related gene sets. These phenotypes indicated that PPM1D-inhibited cells changed into a subtype similar to that present during chronic inflammation, SLE or sepsis, where most neutrophils are polarized into low-density neutrophils［80]. qPCR analysis demonstrated that PPM1D inhibition changed HL-60 cells at the transcriptional level.

In summary, this study demonstrated the effect of a PPM1D inhibitor on myeloid differentiation, its maturation, and the polarization into immunosuppressive neutrophils subsets. Little is known about the target of PPM1D. Chew *et al.* reported that PPM1D is negatively regulated NF-κB signals via the dephosphorylation of S536 in the p65 subunit［81]. The enhancement of inflammation by PPM1D inhibition might be caused by the activation of NF-κB.

The mechanism of the regulation of PPM1D expression level is poorly understood. Zhao's group reported that *Ppm1d*$^{-/-}$*Trp53*$^{-/-}$ mice had similar neutrophil counts to *Ppm1d*$^{-/-}$ mice. This study found that several transcriptional factors might bind to the PPM1D promoter region. List 2-1 contains the transcriptional factors involved in myelopoiesis, for example, C/EBPα, C/EBPβ, C/EBPδ, GATA1, IRF1, and RUNX1.

Interestingly, *Ppm1d* knockout male mice had reduced longevity and exhibited age-associated phenotypes as well as insulin resistance ［82］. Besides, Chen *et al.* (2015) reported that PPM1D expression levels in mice decreased with age ［59］. Our group reported that PPM1D modulated adipogenesis. Diabetes and obesity accelerate aging via inflammation. In elderly, the phagocytotic activity was reduced ［83］.

From these results, a hypothesis was proposed whereby the dephosphorylating capacity of PPM1D decreases with aging and induces immunosenescence and

inflammaging. Thus, understanding how PPM1D expression is controlled requires further study. One possible mechanism is the regulation of PPM1D expression by a humoral factor, pro-inflammatory cytokines, eicosanoids, or exosomes. PPM1D was reported to be hyperactived in tumors and that the frequency of PPM1D mutation increased with age ［57,84］. Hyperactivation of PPM1D may results in obese adipocytes and cancer cells, because a deficiency in PPM1D suppressed the obesity and promoted the autophagy of lipid droplets ［85］. Obese cells secrete pro-inflammatory cytokines ［86］. Therefore, it is possible that PPM1D might have biphasic functions in aging— either as a trigger of inflammaging by the hyperactivation in adipocytes or cancer cells, or as a trigger of immunosenescence by the suppression of immune cells.

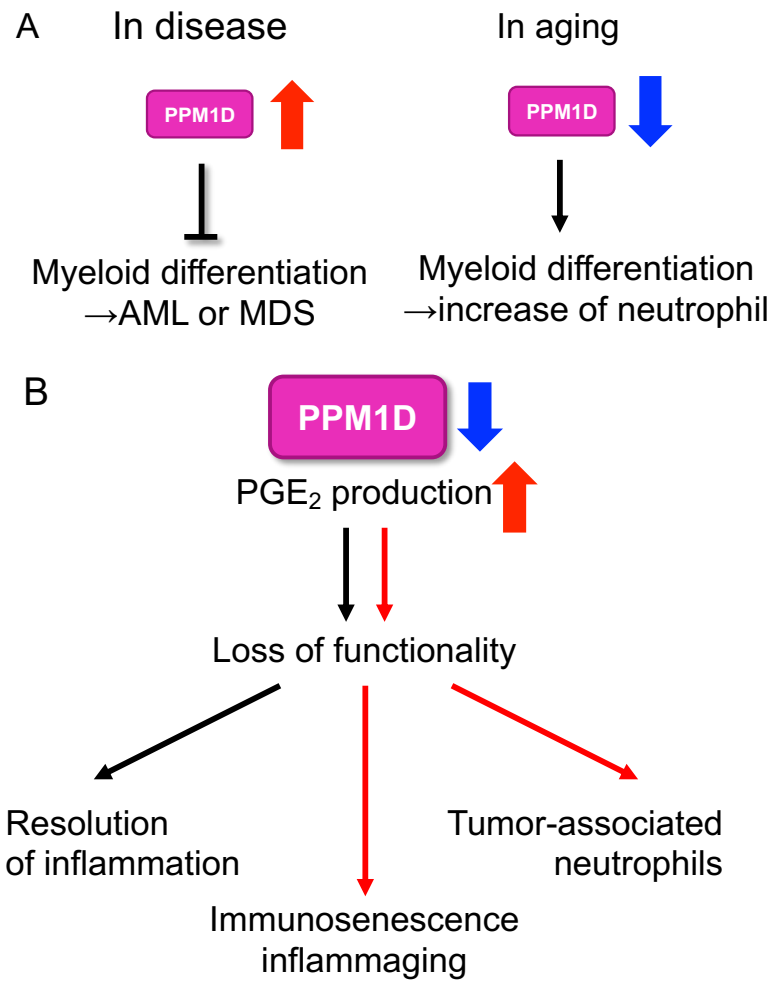

Figure 4-1 The model scheme of decrease of PPM1D expression in myeloid innate immunity

(A) In the chapter 2, it is demonstrated that PPM1D represses myeloid differentiation. In AML and MDS patients, *PPM1D* truncation is observed high frequently. Truncation results in the accumulation of PPM1D, and that repressed differentiation. Furthermore, healthy elderly has increase of neutrophil counts. This phenotype might be caused by decrease of PPM1D with age. (B) In the chapter 3, it is found that PPM1D inhibition induces polarization to immunosuppressive neutrophils. Physiologically resolution of inflammation is induced by PGE_2 production. (Indicated by Black arrows) In elderly people, decrease of PPM1D might induce immunosenescence and tumor-friendly environment (indicated by red arrows).

5. References

1. L. S. Ribeiro, L. Migliari Branco, and B. S. Franklin, Regulation of Innate Immune Responses by Platelets, *Front. Immunol.*, **10**, 1320 (2019).
2. T. Kawasaki and T. Kawai, Toll-like receptor signaling pathways., *Front. Immunol.*, **5**, 461 (2014).
3. Y. Li, H. Zhang, A. K. Kosturakis, R. M. Cassidy, H. Zhang, R. M. Kennamer-Chapman, A. B. Jawad, C. M. Colomand, D. S. Harrison, and P. M. Dougherty, MAPK signaling downstream to TLR4 contributes to paclitaxel-induced peripheral neuropathy., *Brain. Behav. Immun.*, **49**, 255–66 (2015).
4. G. Schabbauer, J. Luyendyk, K. Crozat, Z. Jiang, N. Mackman, S. Bahram, and P. Georgel, TLR4/CD14-mediated PI3K activation is an essential component of interferon-dependent VSV resistance in macrophages, *Mol. Immunol.*, **45**, 2790–2796 (2008).
5. S. J. Galli, N. Borregaard, and T. A. Wynn, Phenotypic and functional plasticity of cells of innate immunity: macrophages, mast cells and neutrophils, *Nat. Immunol.*, **12**, 1035–1044 (2011).
6. G. Schett and M. F. Neurath, Resolution of chronic inflammatory disease: universal and tissue-specific concepts., *Nat. Commun.*, **9**, 3261 (2018).
7. C. A. Loynes, J. A. Lee, A. L. Robertson, M. J. Steel, F. Ellett, Y. Feng, B. D. Levy, M. K. B. Whyte, and S. A. Renshaw, PGE2 production at sites of tissue injury promotes an anti-inflammatory neutrophil phenotype and determines the outcome of inflammation resolution in vivo., *Sci. Adv.*, **4**, eaar8320 (2018).
8. J. L. Schultze and M. Beyer, Myelopoiesis Reloaded: Single-Cell Transcriptomics Leads the Way, *Immunity*, **44**, 18–20 (2016).
9. H. Dombret and C. Gardin, An update of current treatments for adult acute myeloid leukemia, *Blood*, **127**, 53–62 (2015).
10. M. Ozeki, J. E. Shively, and A. Hl-, Differential cell fates induced by all-trans retinoic acid-treated HL-60 human leukemia cells, *J. Leukoc. Biol.*, **84**, (2008).
11. J. Á. Nicolás-Ávila, J. M. Adrover, and A. Hidalgo, Neutrophils in Homeostasis, Immunity, and Cancer, *Immunity*, **46**, 15–28 (2017).
12. R. S. Flannagan, V. Jaumouillé, and S. Grinstein, The cell biology of phagocytosis., *Annu. Rev. Pathol.*, **7**, 61–98 (2012).

13. B. E. Oyinloye, A. F. Adenowo, and A. P. Kappo, Reactive oxygen species, apoptosis, antimicrobial peptides and human inflammatory diseases., *Pharmaceuticals (Basel).*, **8**, 151–75 (2015).
14. C. Tecchio, A. Micheletti, and M. A. Cassatella, Neutrophil-derived cytokines: facts beyond expression., *Front. Immunol.*, **5**, 508 (2014).
15. P. T. Bozza, I. Bakker-Abreu, R. A. Navarro-Xavier, and C. Bandeira-Melo, Lipid body function in eicosanoid synthesis: an update., *Prostaglandins. Leukot. Essent. Fatty Acids*, **85**, 205–13 (2011).
16. R. C. N. Melo, H. D'Avila, H.-C. Wan, P. T. Bozza, A. M. Dvorak, and P. F. Weller, Lipid bodies in inflammatory cells: structure, function, and current imaging techniques., *J. Histochem. Cytochem.*, **59**, 540–56 (2011).
17. H.-C. Wan, R. C. N. Melo, Z. Jin, A. M. Dvorak, and P. F. Weller, Roles and origins of leukocyte lipid bodies: proteomic and ultrastructural studies., *FASEB J.*, **21**, 167–78 (2007).
18. F. Nose, T. Yamaguchi, R. Kato, T. Aiuchi, T. Obama, S. Hara, M. Yamamoto, and H. Itabe, Crucial Role of Perilipin-3 (TIP47) in Formation of Lipid Droplets and PGE2 Production in HL-60-Derived Neutrophils, *PLoS One*, **8**, e71542 (2013).
19. M. A. Giese, L. E. Hind, and A. Huttenlocher, Neutrophil plasticity in the tumor microenvironment, (2019).
20. J. B. G. Mackey, S. B. Coffelt, and L. M. Carlin, Neutrophil Maturity in Cancer, *Front. Immunol.*, **10**, 1912 (2019).
21. Z. Granot, Neutrophils as a Therapeutic Target in Cancer, *Front. Immunol.*, **10**, 1710 (2019).
22. L. G. Ng, R. Ostuni, and A. Hidalgo, Heterogeneity of neutrophils, *Nat. Rev. Immunol.*, **19**, 255–265 (2019).
23. S. Brandau, S. Trellakis, K. Bruderek, D. Schmaltz, G. Steller, M. Elian, H. Suttmann, M. Schenck, J. Welling, P. Zabel, and S. Lang, Myeloid-derived suppressor cells in the peripheral blood of cancer patients contain a subset of immature neutrophils with impaired migratory properties, *J. Leukoc. Biol.*, **89**, 311–317 (2011).
24. A. G. Cuenca, M. J. Delano, K. M. Kelly-Scumpia, C. Moreno, P. O. Scumpia, D. M. LaFace, P. G. Heyworth, P. A. Efron, and L. L. Moldawer, A Paradoxical

Role for Myeloid-Derived Suppressor Cells in Sepsis and Trauma, *Mol. Med.*, **17**, 281–292 (2011).

25. J. Zhou, Y. Nefedova, A. Lei, and D. Gabrilovich, Neutrophils and PMN-MDSC: Their biological role and interaction with stromal cells, *Semin. Immunol.*, **35**, 19–28 (2018).
26. M. I. Cuartero, I. Ballesteros, A. Moraga, F. Nombela, J. Vivancos, J. A. Hamilton, Á. L. Corbí, I. Lizasoain, and M. A. Moro, N2 neutrophils, novel players in brain inflammation after stroke: modulation by the PPARγ agonist rosiglitazone., *Stroke*, **44**, 3498–508 (2013).
27. J. Y. Sagiv, J. Michaeli, S. Assi, I. Mishalian, H. Kisos, L. Levy, P. Damti, D. Lumbroso, L. Polyansky, R. V Sionov, A. Ariel, A.-H. Hovav, E. Henke, Z. G. Fridlender, and Z. Granot, Phenotypic diversity and plasticity in circulating neutrophil subpopulations in cancer., *Cell Rep.*, **10**, 562–73 (2015).
28. X. Huo, H. Li, Z. Li, C. Yan, I. Agrawal, S. Mathavan, J. Liu, and Z. Gong, Transcriptomic profiles of tumor-associated neutrophils reveal prominent roles in enhancing angiogenesis in liver tumorigenesis in zebrafish, *Sci. Rep.*, **9**, 1509 (2019).
29. B. V Kumar, T. J. Connors, and D. L. Farber, Human T Cell Development, Localization, and Function throughout Life., *Immunity*, **48**, 202–213 (2018).
30. R. C. Lynn, E. W. Weber, E. Sotillo, D. Gennert, P. Xu, Z. Good, H. Anbunathan, J. Lattin, R. Jones, V. Tieu, S. Nagaraja, J. Granja, C. F. A. de Bourcy, R. Majzner, A. T. Satpathy, S. R. Quake, M. Monje, H. Y. Chang, and C. L. Mackall, c-Jun overexpression in CAR T cells induces exhaustion resistance, *Nature*, **576**, 293–300 (2019).
31. A. Ponzetta, R. Carriero, S. Carnevale, M. Barbagallo, M. Molgora, C. Perucchini, E. Magrini, F. Gianni, P. Kunderfranco, N. Polentarutti, F. Pasqualini, S. Di Marco, D. Supino, C. Peano, F. Cananzi, P. Colombo, S. Pilotti, S. Y. Alomar, E. Bonavita, M. R. Galdiero, C. Garlanda, A. Mantovani, and S. Jaillon, Neutrophils Driving Unconventional T Cells Mediate Resistance against Murine Sarcomas and Selected Human Tumors., *Cell*, **178**, 346-360.e24 (2019).
32. C. Silvestre-Roig, A. Hidalgo, and O. Soehnlein, Neutrophil heterogeneity: implications for homeostasis and pathogenesis, *Blood*, **127**, 2173–2181 (2016).

33. F. Veglia, V. A. Tyurin, M. Blasi, A. De Leo, A. V. Kossenkov, L. Donthireddy, T. K. J. To, Z. Schug, S. Basu, F. Wang, E. Ricciotti, C. DiRusso, M. E. Murphy, R. H. Vonderheide, P. M. Lieberman, C. Mulligan, B. Nam, N. Hockstein, G. Masters, M. Guarino, C. Lin, Y. Nefedova, P. Black, V. E. Kagan, and D. I. Gabrilovich, Fatty acid transport protein 2 reprograms neutrophils in cancer, *Nature*, **569**, 73–78 (2019).
34. D. L. Brautigan, Protein Ser/Thr phosphatases--the ugly ducklings of cell signalling., *FEBS J.*, **280**, 324–45 (2013).
35. D. L. Brautigan and S. Shenolikar, Protein Serine/Threonine Phosphatases: Keys to Unlocking Regulators and Substrates, *Annu. Rev. Biochem.*, **87**, 921–964 (2018).
36. J. V. Olsen, B. Blagoev, F. Gnad, B. Macek, C. Kumar, P. Mortensen, and M. Mann, Global, In Vivo, and Site-Specific Phosphorylation Dynamics in Signaling Networks, *Cell*, **127**, 635–648 (2006).
37. Y. Shi, Serine/Threonine Phosphatases: Mechanism through Structure, *Cell*, **139**, 468–484 (2009).
38. M. Fiscella, H. Zhang, S. Fan, K. Sakaguchi, S. Shen, W. E. Mercer, G. F. Vande Woude, P. M. O'Connor, and E. Appella, Wip1, a novel human protein phosphatase that is induced in response to ionizing radiation in a p53-dependent manner., *Proc. Natl. Acad. Sci. U. S. A.*, **94**, 6048–53 (1997).
39. Y. Chuman, W. Kurihashi, Y. Mizukami, T. Nashimoto, H. Yagi, and K. Sakaguchi, PPM1D430, a novel alternative splicing variant of the human PPM1D, can dephosphorylate p53 and exhibits specific tissue expression, *J. Biochem.*, **145**, 1–12 (2009).
40. E. Ruark, K. Snape, P. Humburg, C. Loveday, I. Bajrami, R. Brough, D. N. Rodrigues, A. Renwick, S. Seal, E. Ramsay, S. D. V. Duarte, M. A. Rivas, M. Warren-Perry, A. Zachariou, A. Campion-Flora, S. Hanks, A. Murray, N. A. Pour, J. Douglas, L. Gregory, A. Rimmer, N. M. Walker, T.-P. Yang, J. W. Adlard, J. Barwell, J. Berg, A. F. Brady, C. Brewer, G. Brice, C. Chapman, J. Cook, R. Davidson, A. Donaldson, F. Douglas, D. Eccles, D. G. Evans, L. Greenhalgh, A. Henderson, L. Izatt, A. Kumar, F. Lalloo, Z. Miedzybrodzka, P. J. Morrison, J. Paterson, M. Porteous, M. T. Rogers, S. Shanley, L. Walker, M. Gore, R. Houlston, M. A. Brown, M. J. Caufield, P. Deloukas, M. I. McCarthy, J.

A. Todd, C. Turnbull, J. S. Reis-Filho, A. Ashworth, A. C. Antoniou, C. J. Lord, P. Donnelly, N. Rahman, P. Donnelly, and N. Rahman, Mosaic PPM1D mutations are associated with predisposition to breast and ovarian cancer, *Nature*, **493**, 406–410 (2012).

41. G. Genovese, A. K. Kähler, R. E. Handsaker, J. Lindberg, S. a. Rose, S. F. Bakhoum, K. Chambert, E. Mick, B. M. Neale, M. Fromer, S. M. Purcell, O. Svantesson, M. Landén, M. Höglund, S. Lehmann, S. B. Gabriel, J. L. Moran, E. S. Lander, P. F. Sullivan, P. Sklar, H. Grönberg, C. M. Hultman, and S. a. McCarroll, Clonal Hematopoiesis and Blood-Cancer Risk Inferred from Blood DNA Sequence., *N. Engl. J. Med.*, **371**, 141126135947008 (2014).
42. R. C. Lindsley, W. Saber, B. G. Mar, R. Redd, T. Wang, M. D. Haagenson, P. V. Grauman, Z.-H. Hu, S. R. Spellman, S. J. Lee, M. R. Verneris, K. Hsu, K. Fleischhauer, C. Cutler, J. H. Antin, D. Neuberg, and B. L. Ebert, Prognostic Mutations in Myelodysplastic Syndrome after Stem-Cell Transplantation, *N. Engl. J. Med.*, **376**, 536–547 (2017).
43. M. Richter, T. Dayaram, A. G. Gilmartin, G. Ganji, S. K. Pemmasani, H. Van Der Key, J. M. Shohet, L. A. Donehower, and R. Kumar, WIP1 phosphatase as a potential therapeutic target in neuroblastoma., *PLoS One*, **10**, e0115635 (2015).
44. H. Yagi, Y. Chuman, Y. Kozakai, T. Imagawa, Y. Takahashi, F. Yoshimura, K. Tanino, and K. Sakaguchi, A small molecule inhibitor of p53-inducible protein phosphatase PPM1D, *Bioorg. Med. Chem. Lett.*, **22**, 729–732 (2012).
45. S. Ogasawara, Y. Kiyota, Y. Chuman, A. Kowata, F. Yoshimura, K. Tanino, R. Kamada, and K. Sakaguchi, Novel inhibitors targeting PPM1D phosphatase potently suppress cancer cell proliferation., *Bioorg. Med. Chem.*, **23**, 6246–9 (2015).
46. S. Shreeram, W. K. Hee, O. N. Demidov, C. Kek, H. Yamaguchi, A. J. Fornace, C. W. Anderson, E. Appella, and D. V. Bulavin, Regulation of ATM/p53-dependent suppression of myc-induced lymphomas by Wip1 phosphatase, *J. Exp. Med.*, **203**, 2793–2799 (2006).
47. X. Lu, D. Bocangel, B. Nannenga, H. Yamaguchi, E. Appella, and L. A. Donehower, The p53-Induced Oncogenic Phosphatase PPM1D Interacts with Uracil DNA Glycosylase and Suppresses Base Excision Repair, *Mol. Cell*, **15**, 621–634 (2004).

48. G. Mönke, E. Cristiano, A. Finzel, D. Friedrich, H. Herzel, M. Falcke, and A. Loewer, Excitability in the p53 network mediates robust signaling with tunable activation thresholds in single cells, *Sci. Rep.*, **7**, 46571 (2017).
49. J. Choi, B. Nannenga, O. N. Demidov, D. V Bulavin, A. Cooney, C. Brayton, Y. Zhang, I. N. Mbawuike, A. Bradley, E. Appella, and L. A. Donehower, Mice deficient for the wild-type p53-induced phosphatase gene (Wip1) exhibit defects in reproductive organs, immune function, and cell cycle control., *Mol. Cell. Biol.*, **22**, 1094–105 (2002).
50. Y. Kozakai, R. Kamada, J. Furuta, Y. Kiyota, Y. Chuman, and K. Sakaguchi, PPM1D controls nucleolar formation by up-regulating phosphorylation of nucleophosmin, *Sci. Rep.*, **6**, 33272 (2016).
51. G. Liu, X. Hu, B. Sun, T. Yang, J. Shi, L. Zhang, and Y. Zhao, Phosphatase Wip1 negatively regulates neutrophil development through p38 MAPK-STAT1, *Blood*, **121**, 519–529 (2013).
52. S. Ogasawara, Y. Chuman, T. Michiba, R. Kamada, T. Imagawa, and K. Sakaguchi, Inhibition of protein phosphatase PPM1D enhances retinoic acid-induced differentiation in human embryonic carcinoma cell line, *J. Biochem.*, **165**, 471–477 (2019).
53. R. Kamada, N. Kimura, F. Yoshimura, K. Tanino, and K. Sakaguchi, Inhibition of lipid droplet formation by Ser/Thr protein phosphatase PPM1D inhibitor, SL-176, *PLoS One*, **14**, e0212682 (2019).
54. J. Xia, C. A. Miller, J. Baty, A. Ramesh, M. R. M. Jotte, R. S. Fulton, T. P. Vogel, M. A. Cooper, K. J. Walkovich, V. Makaryan, A. A. Bolyard, M. C. Dinauer, D. B. Wilson, A. Vlachos, K. C. Myers, R. J. Rothbaum, A. A. Bertuch, D. C. Dale, A. Shimamura, L. A. Boxer, and D. C. Link, Somatic mutations and clonal hematopoiesis in congenital neutropenia., *Blood*, **131**, 408–416 (2018).
55. P. Kleiblova, I. A. Shaltiel, J. Benada, J. ??ev????k, S. Pech????kov??, P. Pohlreich, E. E. Voest, P. Dundr, J. Bartek, Z. Kleibl, R. H. Medema, and L. Macurek, Gain-of-function mutations of PPM1D/Wip1 impair the p53-dependent G1 checkpoint, *J. Cell Biol.*, **201**, 511–521 (2013).
56. A. Zajkowicz, D. Butkiewicz, A. Drosik, M. Giglok, R. Suwiński, and M. Rusin, Truncating mutations of PPM1D are found in blood DNA samples of lung cancer patients, *Br. J. Cancer*, **112**, 1114–1120 (2015).

57. S. Jaiswal, P. Fontanillas, J. Flannick, A. Manning, P. V. Grauman, B. G. Mar, R. C. Lindsley, C. H. Mermel, N. Burtt, A. Chavez, J. M. Higgins, V. Moltchanov, F. C. Kuo, M. J. Kluk, B. Henderson, L. Kinnunen, H. A. Koistinen, C. Ladenvall, G. Getz, A. Correa, B. F. Banahan, S. Gabriel, S. Kathiresan, H. M. Stringham, M. I. McCarthy, M. Boehnke, J. Tuomilehto, C. Haiman, L. Groop, G. Atzmon, J. G. Wilson, D. Neuberg, D. Altshuler, and B. L. Ebert, Age-Related Clonal Hematopoiesis Associated with Adverse Outcomes, *N. Engl. J. Med.*, **371**, 2488–2498 (2014).

58. J. I. Hsu, T. Dayaram, A. Tovy, E. De Braekeleer, M. Jeong, F. Wang, J. Zhang, T. P. Heffernan, S. Gera, J. J. Kovacs, J. R. Marszalek, C. Bristow, Y. Yan, G. Garcia-Manero, H. Kantarjian, G. Vassiliou, P. A. Futreal, L. A. Donehower, K. Takahashi, and M. A. Goodell, PPM1D Mutations Drive Clonal Hematopoiesis in Response to Cytotoxic Chemotherapy., *Cell Stem Cell*, **23**, 700-713.e6 (2018).

59. Z. Chen, W. Yi, Y. Morita, H. Wang, Y. Cong, J.-P. Liu, Z. Xiao, K. L. Rudolph, T. Cheng, and Z. Ju, Wip1 deficiency impairs haematopoietic stem cell function via p53 and mTORC1 pathways., *Nat. Commun.*, **6**, 6808 (2015).

60. S. J. Collins, K. A. Robertson, and L. Mueller, Retinoic acid-induced granulocytic differentiation of HL-60 myeloid leukemia cells is mediated directly through the retinoic acid receptor (RAR-alpha)., *Mol. Cell. Biol.*, **10**, 2154–2163 (1990).

61. G. Rovera, D. Santoli, and C. Damsky, Human promyelocytic leukemia cells in culture differentiate into macrophage-like cells when treated with a phorbol diester, **76**, 2779–2783 (1979).

62. S. J. Collins, The HL-60 promyelocytic leukemia cell line: proliferation, differentiation, and cellular oncogene expression., *Blood*, **70**, 1233–44 (1987).

63. S. Oki, T. Ohta, G. Shioi, H. Hatanaka, O. Ogasawara, Y. Okuda, H. Kawaji, R. Nakaki, J. Sese, and C. Meno, Ch IP -Atlas: a data-mining suite powered by full integration of public Ch IP -seq data, *EMBO Rep.*, **19**, (2018).

64. a L. Olins, H. Herrmann, P. Lichter, and D. E. Olins, Retinoic acid differentiation of HL-60 cells promotes cytoskeletal polarization., *Exp. Cell Res.*, **254**, 130–42 (2000).

65. H. Y. Kueh, A. Champhekar, A. Champhekhar, S. L. Nutt, M. B. Elowitz, and E. V Rothenberg, Positive feedback between PU.1 and the cell cycle controls myeloid differentiation., *Science*, **341**, 670–3 (2013).
66. R. M. Zucker, K. Whittington, and B. J. Price, Differentiation of HL-60 cells: cell volume and cell cycle changes., *Cytometry*, **3**, 414–8 (1983).
67. A. Mantovani, M. a Cassatella, C. Costantini, and S. Jaillon, Neutrophils in the activation and regulation of innate and adaptive immunity., *Nat. Rev. Immunol.*, **11**, 519–31 (2011).
68. J. Kargl, S. E. Busch, G. H. Y. Yang, K.-H. Kim, M. L. Hanke, H. E. Metz, J. J. Hubbard, S. M. Lee, D. K. Madtes, M. W. McIntosh, and A. M. Houghton, Neutrophils dominate the immune cell composition in non-small cell lung cancer, *Nat. Commun.*, **8**, 14381 (2017).
69. K. Moses and S. Brandau, Human neutrophils: Their role in cancer and relation to myeloid-derived suppressor cells, *Semin. Immunol.*, **28**, 187–196 (2016).
70. F. Veglia, V. A. Tyurin, M. Blasi, A. De Leo, A. V Kossenkov, L. Donthireddy, K. Jerrick To, Z. Schug, S. Basu, F. Wang, E. Ricciotti, C. Dirusso, M. E. Murphy, H. Vonderheide, P. M. Lieberman, C. Mulligan, B. Nam, N. Hockstein, G. Masters, M. Guarino, C. Lin, Y. Nefedova, P. Black, V. E. Kagan, and D. I. Gabrilovich, Fatty acid transport protein 2 reprograms neutrophils in cancer.
71. V. Prima, L. N. Kaliberova, S. Kaliberov, D. T. Curiel, and S. Kusmartsev, COX2/mPGES1/PGE2 pathway regulates PD-L1 expression in tumor-associated macrophages and myeloid-derived suppressor cells, *Proc. Natl. Acad. Sci.*, **114**, 1117–1122 (2017).
72. D. Kim, J. M. Paggi, C. Park, C. Bennett, and S. L. Salzberg, Graph-based genome alignment and genotyping with HISAT2 and HISAT-genotype, *Nat. Biotechnol.*, **37**, 907–915 (2019).
73. M. Pertea, G. M. Pertea, C. M. Antonescu, T.-C. Chang, J. T. Mendell, and S. L. Salzberg, StringTie enables improved reconstruction of a transcriptome from RNA-seq reads, *Nat. Biotechnol.*, **33**, 290–295 (2015).
74. D. J. McCarthy, Y. Chen, and G. K. Smyth, Differential expression analysis of multifactor RNA-Seq experiments with respect to biological variation, *Nucleic Acids Res.*, **40**, 4288–4297 (2012).

75. A. Paunel-Görgülü, T. Kirichevska, T. Lögters, J. Windolf, and S. Flohé, Molecular Mechanisms Underlying Delayed Apoptosis in Neutrophils from Multiple Trauma Patients with and without Sepsis, *Mol. Med.*, **18**, 325–335 (2012).
76. Z. G. Fridlender, J. Sun, S. Kim, V. Kapoor, G. Cheng, L. Ling, G. S. Worthen, and S. M. Albelda, Polarization of Tumor-Associated Neutrophil Phenotype by TGF-β: "N1" versus "N2" TAN, *Cancer Cell*, **16**, 183–194 (2009).
77. D. Wang and R. N. DuBois, Eicosanoids and cancer, *Nat. Rev. Cancer*, **10**, 181–193 (2010).
78. M. V. Kuleshov, M. R. Jones, A. D. Rouillard, N. F. Fernandez, Q. Duan, Z. Wang, S. Koplev, S. L. Jenkins, K. M. Jagodnik, A. Lachmann, M. G. McDermott, C. D. Monteiro, G. W. Gundersen, and A. Ma'ayan, Enrichr: a comprehensive gene set enrichment analysis web server 2016 update, *Nucleic Acids Res.*, **44**, W90–W97 (2016).
79. A. S. Cowburn, J. Deighton, S. R. Walmsley, and E. R. Chilvers, The survival effect of TNF-α in human neutrophils is mediated via NF-κB-dependent IL-8 release, *Eur. J. Immunol.*, **34**, 1733–1743 (2004).
80. E. Villanueva, S. Yalavarthi, C. C. Berthier, J. B. Hodgin, R. Khandpur, A. M. Lin, C. J. Rubin, W. Zhao, S. H. Olsen, M. Klinker, D. Shealy, M. F. Denny, J. Plumas, L. Chaperot, M. Kretzler, A. T. Bruce, and M. J. Kaplan, Netting Neutrophils Induce Endothelial Damage, Infiltrate Tissues, and Expose Immunostimulatory Molecules in Systemic Lupus Erythematosus, *J. Immunol.*, **187**, 538–552 (2011).
81. J. Chew, S. Biswas, S. Shreeram, M. Humaidi, E. T. Wong, M. K. Dhillion, H. Teo, A. Hazra, C. C. Fang, E. López-Collazo, D. V Bulavin, and V. Tergaonkar, WIP1 phosphatase is a negative regulator of NF-kappaB signalling., *Nat. Cell Biol.*, **11**, 659–66 (2009).
82. H. L. Armata, S. Chamberland, L. Watts, H. J. Ko, Y. Lee, D. Y. Jung, J. K. Kim, and H. K. Sluss, Deficiency of the tumor promoter gene wip1 induces insulin resistance., *Mol. Endocrinol.*, **29**, 28–39 (2015).
83. R. R. Montgomery and A. C. Shaw, Paradoxical changes in innate immunity in aging: recent progress and new directions., *J. Leukoc. Biol.*, **98**, 937–43 (2015).

84. M. Xie, C. Lu, J. Wang, M. D. McLellan, K. J. Johnson, M. C. Wendl, J. F. McMichael, H. K. Schmidt, V. Yellapantula, C. A. Miller, B. A. Ozenberger, J. S. Welch, D. C. Link, M. J. Walter, E. R. Mardis, J. F. Dipersio, F. Chen, R. K. Wilson, T. J. Ley, and L. Ding, Age-related mutations associated with clonal hematopoietic expansion and malignancies., *Nat. Med.*, **20**, 1472–8 (2014).

85. X. Le Guezennec, A. Brichkina, Y.-F. Huang, E. Kostromina, W. Han, and D. V. Bulavin, Wip1-Dependent Regulation of Autophagy, Obesity, and Atherosclerosis, *Cell Metab.*, **16**, 68–80 (2012).

86. M. A. McArdle, O. M. Finucane, R. M. Connaughton, A. M. McMorrow, and H. M. Roche, Mechanisms of Obesity-Induced Inflammation and Insulin Resistance: Insights into the Emerging Role of Nutritional Strategies, *Front. Endocrinol. (Lausanne).*, **4**, 52 (2013).

6. Acknowledgement

I would like to express my gratitude to my supervisor Prof. Kazuyasu Sakaguchi for the continuous support of my study in Laboratory of Biological Chemistry. His advice and comments helped me in all the time of research. Besides, I had great opportunities to grow up not only as a researcher but also as a member of society thanks to his help.

Besides my supervisor, I would like to offer my special thanks to Professor Yota Murakami (Laboratory of Bioorganic Chemistry), Professor Mutsumi Takagi (Laboratory of Cell Processing Engineering, Faculty of Engineering), Professor Keiji Tanino (Laboratory of Organic Chemistry II), Professor Akinori Takaoka (Division of Signaling in Cancer and Immunology) for their insightful comments and encouragement.

I am grateful to Professor Keiji Tanino who provided PPM1D inhibitor series and TAP-4PH, Professor Shuji Shigenobu (National Institute for Basic Biology) who collaborate in transcriptome analysis, and also Professor Murakami and Professor Takaoka who gave me the opportunity to perform transfection in their lab. For using the Flow cytometer and Quantitative PCR analyzer I was supported by Global Facility center (GFC), Pharma Science Open Unit (PSOU), funded by MEXT and AMED. Besides, I offer my thanks to Professor Gerardo Ferbeyre and Dr. Frederick Lessard (Département de biochimie, Faculté de Médecine, Université de Montréal, QC, Canada) inspired me.

With great esteem, gratitude, and respect, I express my heartfelt obligations to Assistant professor Rui Kamada (Laboratory of Biological Chemistry). Her distinguished supervising guide, excellent teaching and constant encouragement for my research always supported me to writing thesis from the beginning to work. And also, she taught me the responsibilities as a senior and member of society. Her role will remain as an origin of my inspiration as a researcher throughout my life. I strongly hope her to mentor me for years to come. And Associate Professor Toshiaki Imagawa gave me many advices, and secretary Michiko Taniguchi always helps me a lot.

And also, I thank my fellow lab mates in for the stimulating discussions, Dr. Kozakai, Dr. Sakaguchi, Dr. Wada, Dr. Kiyota, Dr. Toguchi, Ms. Shirahata, Ms. Tanno, Mr. Furuta, Dr. Ogasawara, Ms. Kanno, Mr. Sasaki, Ms. Tsukahara, Ms. Nakagawa, Ms. Nakayama, Mr. Mine, and all junior lab mates. Especially, I greatly appreciate Dr. Ogasawara's advice, supports and teaching. Especially on my thesis, Mr. Ito and Mr. Iikura do tough works together in HL-60 differentiation experiments, and the literature searched by Ms. Tashiro greatly helped me in the last part of chapter 3. And also, it is fun for me to research about PPM1D with Mr. Kawamura, Ms. Tani, Ms. Ushio, Ms. Uno and Mr. Tsukamoto.

This study was supported by JSPS KAKENHI Grant Number 18J11499, 17K17565.

Last but not least, I would like to thank my family: my father Hiroshi, my mother Yukari and Kazutoshi for supporting me throughout research and my life in general.

Η ΑΛΗΘΕΙΑ ΕΛΕΥΘΕΡΩΣΕΙ ΥΜΑΣ.

----Ιωάννης 8:32